

14. SITE 458: MARIANA FORE-ARC¹

Shipboard Scientific Party²

HOLE 458

Date occupied: 18 April, 1978

Date departed: 22 April, 1978

Time on hole: 103 hours 12 minutes

Position (latitude; longitude): 17°51.85'N; 146°56.06'E

Water depth (sea level; corrected m, echo-sounding): 3453

Water depth (rig floor; corrected m, echo-sounding): 3463

Bottom felt (m, drill pipe): 3459

Penetration (m): 465.5

Number of holes: 1

Number of cores: 49

Total length of cored section (m): 465.5

Total core recovered (m): 97.83

Core recovery (%): 21.0

Oldest sediment cored:

Depth sub-bottom (m): ~250

Nature: siltstone and sandstone

Age: early Oligocene

Measured velocity (km/s): 1.9–2.5

Basement:

Depth sub-bottom (m): 256.5

Nature: bronzite andesite and tholeiitic basalt

Velocity range (km/s): 3.2–4.7

Total penetration (m): 209

Principal results: Site 458, the first drill site of the Mariana fore-arc series, is located on the southeast periphery of a 40-mgal positive gravity anomaly between the trench axis and the active volcanic arc. The site objectives included determining the sedimentary history and the nature and origin of the basement in the Mariana fore-arc region. Of the total penetration of 465.5 meters (core recovery rate 21%), the upper 256.5 meters comprises sediments consisting mainly of siliceous nannofossil foraminifer ooze and vitric mud (0–95 m), nannofossil chalk (95–247 m) and laminated graded vitric siltstone and sandstone (247–256.5 m). The oldest sediments are early Oligocene in age. Sedimentation was interrupted by one major (4-m.y.) hiatus in the late Miocene and early Pliocene, and three lesser hiatuses. Supply of volcanic ash from successive volcanic arcs to the west (the Palau-Kyushu Ridge, the West Mariana Ridge, and the present Mariana arc) occurred vir-

tually without interruption, although ash levels were highest in the early Oligocene and in the Plio-Pleistocene.

Basement rocks recovered are pillows and massive volcanic flows comprising four distinct petrographic and geochemical types. The upper type (256.6–380 m sub-bottom) is mainly aphyric, two-pyroxene, high-MgO andesite, and is normally magnetized. These lavas include peculiar glassy rocks of the boninite suite having magnesian orthopyroxene (bronzite) microphenocrysts, abundant acicular clinopyroxene, and no plagioclase. The lower three types (380–465.5 m sub-bottom) are reversely magnetized, highly fractured and altered augite-plagioclase basalt, high-MgO andesite, and augite-plagioclase basalt, in order of depth. There are no fault-produced repetitions of lava types.

Heat flow at the site is estimated at 0.6 HFU. Downhole logging was not possible for lack of a bit release sub-assembly.

BACKGROUND AND OBJECTIVES

Site 458 is in the middle of the Mariana fore-arc region, ~85 km west of the axis of the Mariana Trench and ~130 km east of the active volcanic islands (Figs. 1–4). The hole is the first of a series that includes Sites 460 and 461, deep on the island-arc wall of the trench, and Site 459, at the eastern edge of the first fore-arc basin sediments adjacent to the trench slope break (Fig. 2). General background and objectives and drilling in the Mariana fore-arc region are summarized in a separate chapter. Here, only the background and objectives specific to Site 458 are given.

Site 458 was an alternative site in the Leg 60 pre-cruise drilling plan. It was selected to be near the large gravity anomaly centered near 17°54'N and 146°52'E on Figure 5. For a complete description of the geophysical setting and Site 458, see Hussong and Fryer, this

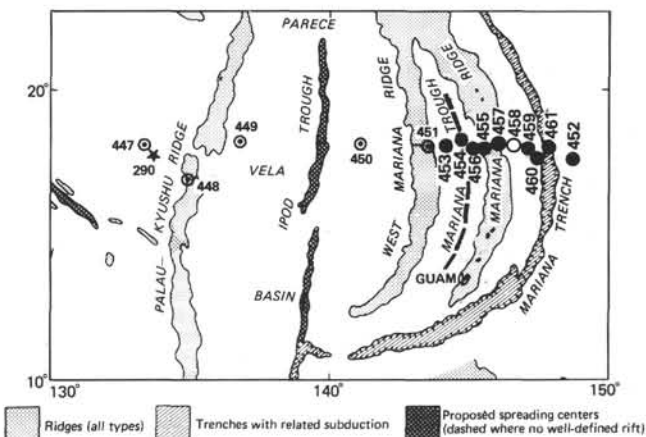


Figure 1. Location of Site 458 (open circle) in the Mariana fore-arc region. Other Leg 60 sites are closed circles. Sites drilled on Leg 59 are shown by circled dots. Site 290 (Leg 31) is shown by a star.

¹ Initial Reports of the Deep Sea Drilling Project, Volume 60.

² Donald M. Hussong (Co-Chief Scientist), Hawaii Institute of Geophysics, Honolulu, Hawaii; Seiya Uyeda (Co-Chief Scientist), Earthquake Research Institute, University of Tokyo, Tokyo, Japan; René Blanchet, Université de Bretagne Occidentale, Brest, France; Ulrich Bleil, Institut für Geophysik, Ruhr Universität, Bochum, Federal Republic of Germany; C. Howard Ellis, Marathon Oil Company, Denver Research Center, Littleton, Colorado; Timothy J. G. Francis, Institute of Oceanographic Sciences, Surrey, United Kingdom; Patricia Fryer, Hawaii Institute of Geophysics, Honolulu, Hawaii; Ki-Iti Horai, Lamont-Doherty Geological Observatory, Palisades, New York; Stanley Kling, Marine Life Research Group, Scripps Institution of Oceanography, La Jolla, California (present address: 416 Shore View Lane, Leucadia, California); Arend Meijer, Department of Geosciences, University of Arizona, Tucson, Arizona; Kazuaki Nakamura, Earthquake Research Institute, University of Tokyo, Tokyo, Japan; James H. Natland, Deep Sea Drilling Project, Scripps Institution of Oceanography, La Jolla, California; Gordon H. Packham, Department of Geology and Geophysics, University of Sydney, Sydney, N.S.W. Australia; and Anatoly Sharaskin, Vernadsky Institute of Geochemistry, U.S.S.R. Academy of Sciences, Moscow, U.S.S.R.

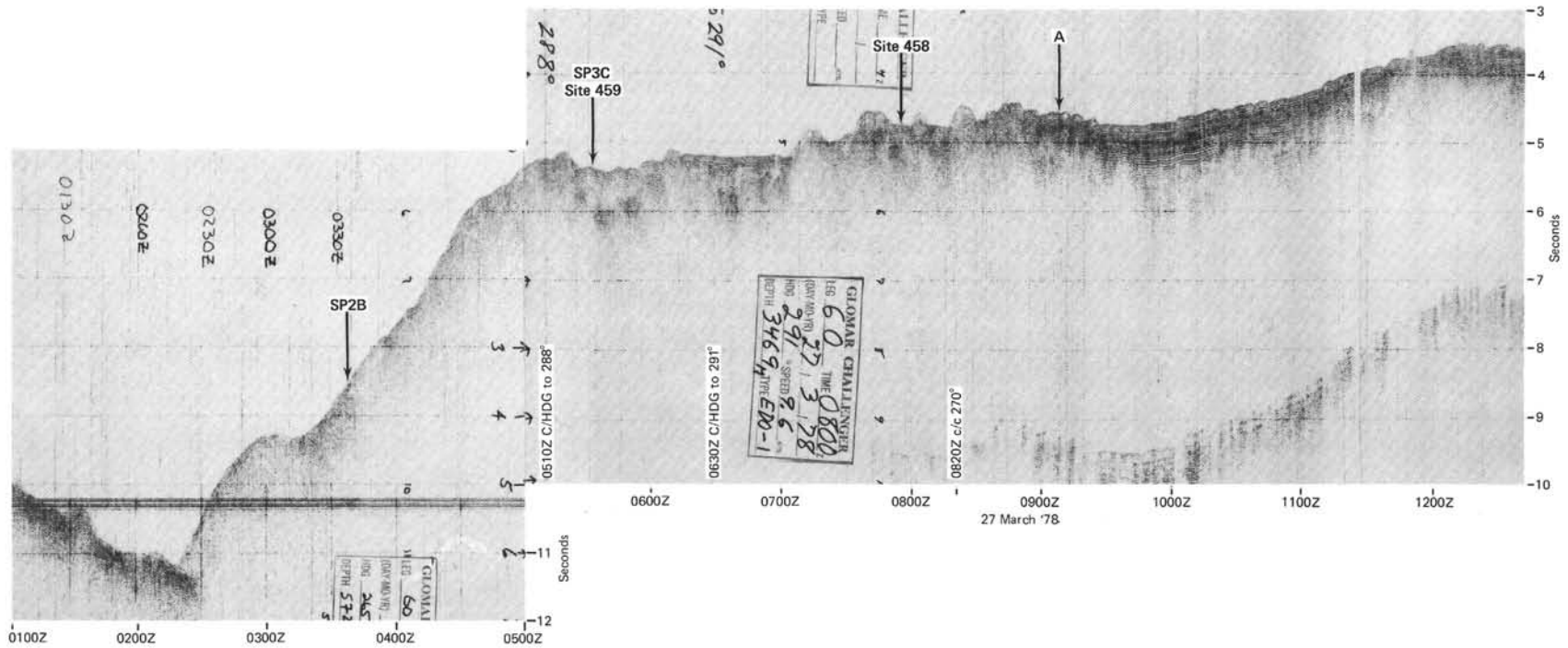


Figure 2. *Glomar Challenger* reflection profile approaching Site 458 from the Mariana Trench. Site locations are close to, but not on, this line. Locations shown here are projected (see Fig. 3 for site locations).

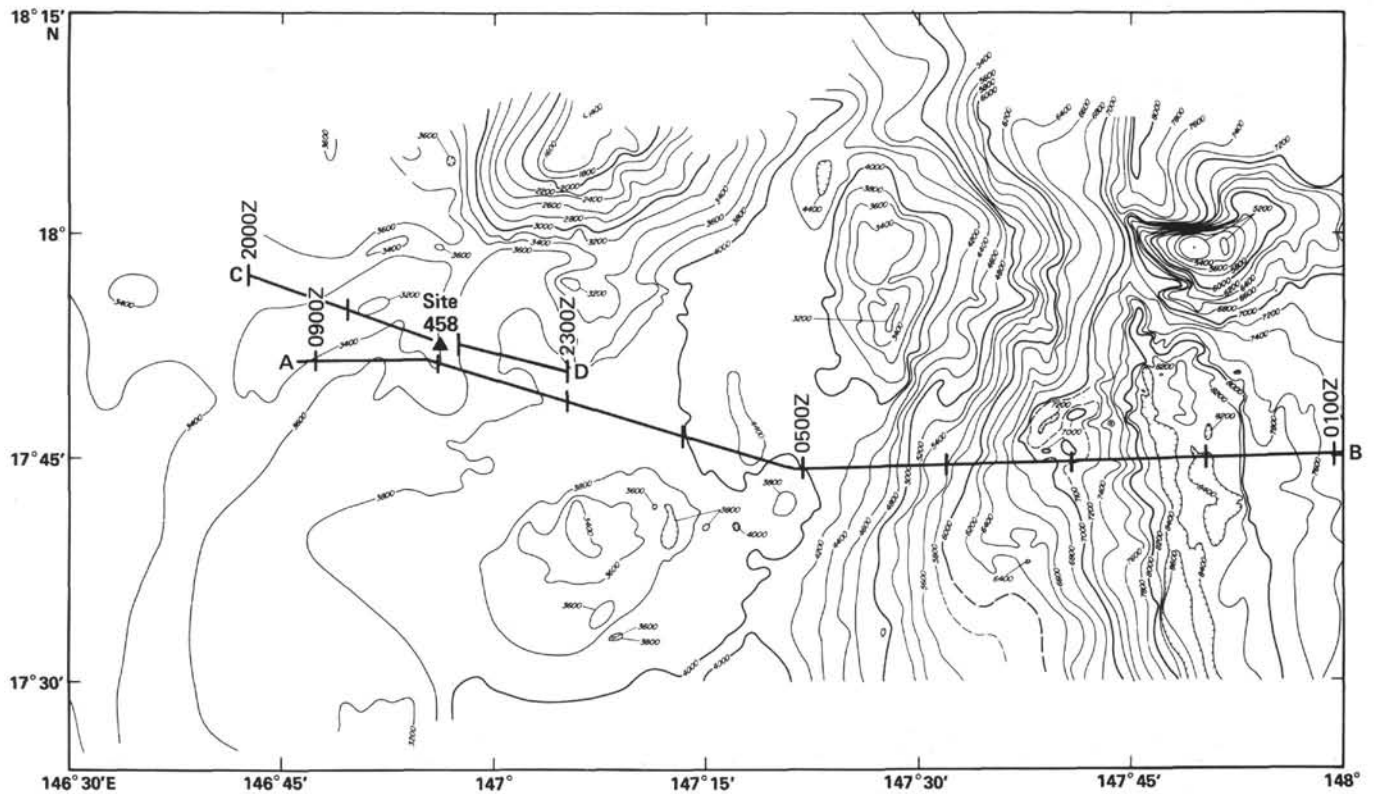


Figure 3. Bathymetry of the fore-arc region near Site 458, from Hussong (this volume). Track A-B is Figure 2. Track C-D is Figure 4.

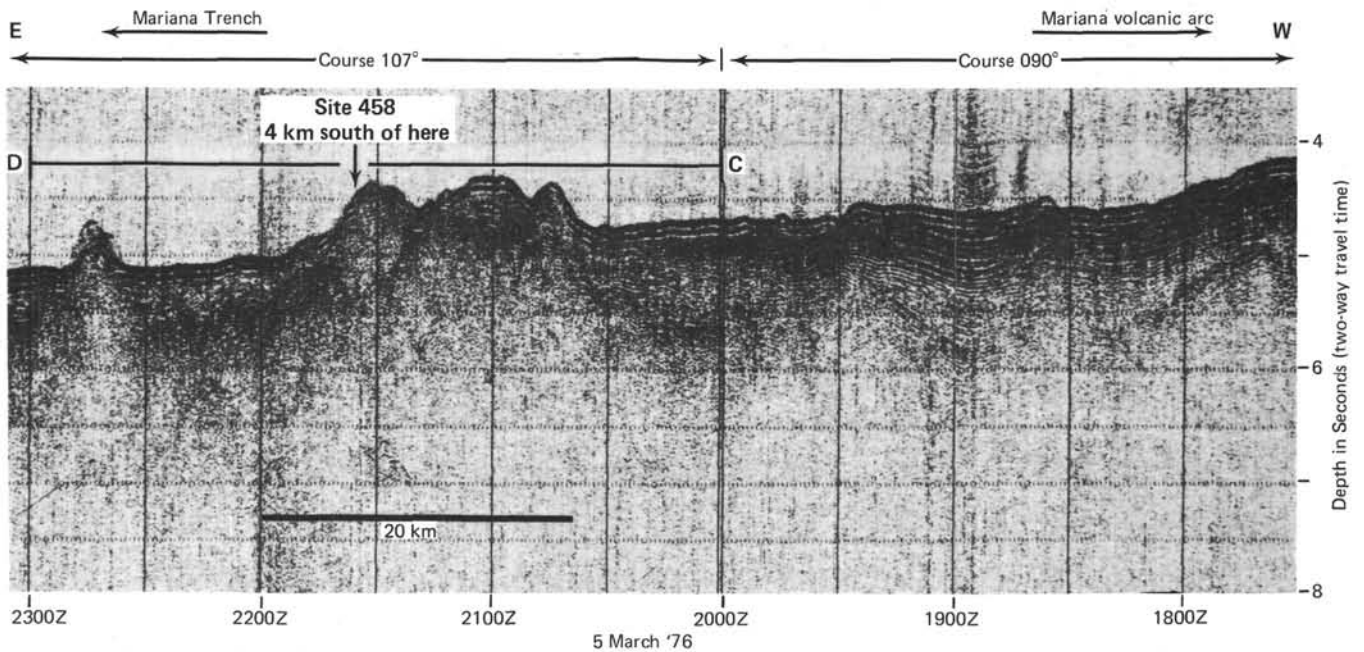


Figure 4. Portion of Hawaii Institute of Geophysics site survey airgun reflection seismic profile obtained on 5 March 1976. Single-channel hydrophone array, filtered 20-80 Hz. Track C-D is shown on Figure 3.

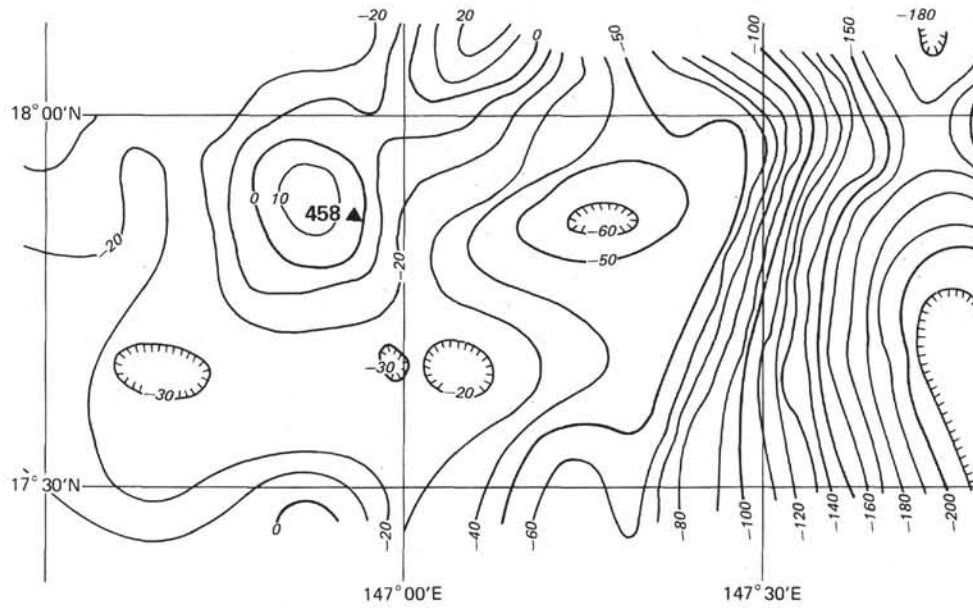


Figure 5. Free-air gravity anomaly near Site 458 (from Plate 1, Hussong, this volume). Positive anomaly discussed in the text is near 17° 53' N, 146° 53' E. Contour interval is 10 mgals.

volume. The anomalous body responsible for the gravity high also causes an apparent magnetic dipole (Fig. 6), yet has very little bathymetric expression (Fig. 3). Refraction data (LaTraille and Hussong, 1980) near the anomaly suggest that beneath the seafloor at Site 458 there is about one km of sediments (velocity 2.4–3.5 km/s), underlain by another 2.5 km of material with velocities of 3.5 to 5 km/s, before velocities rise to over 6

km/s at about 3.5-km sub-bottom. However, if these low-velocity, and thus presumably low-density, materials are widespread around Site 458, to satisfy the gravity data a model is required that employs something similar to a cone of the 6-km/s material, with a base of less than 10-km diameter and a 5° slope, rising through the sediments to near the seafloor. Gravity models are not unique, of course, so an infinite variety of shapes,

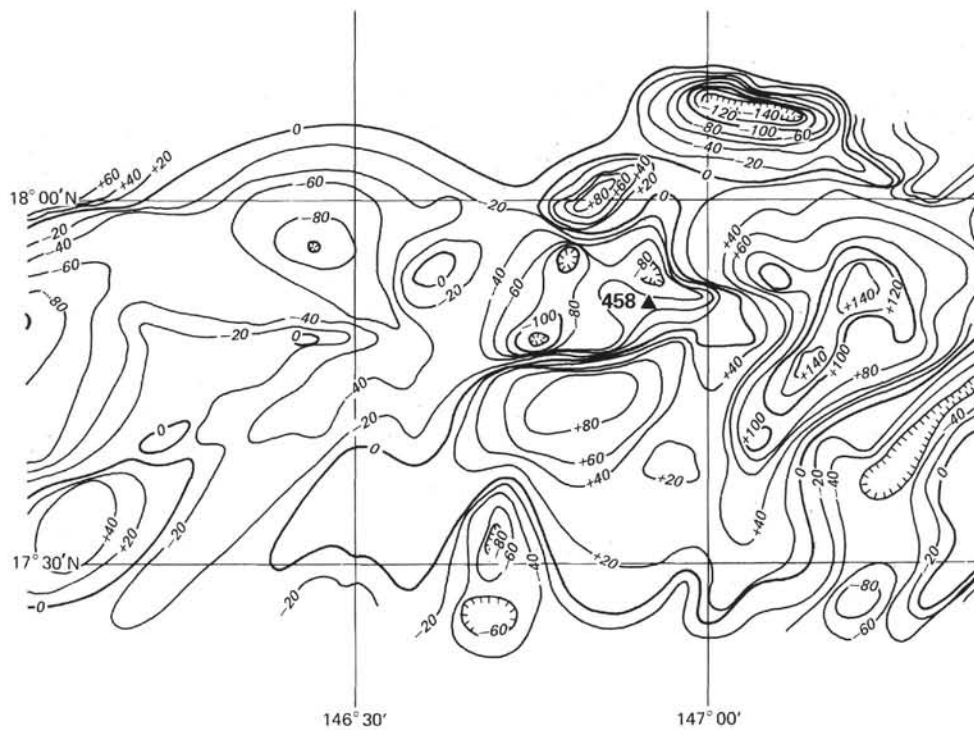


Figure 6. Magnetic anomalies near Site 458 (from Plate 1, Hussong, this volume).

depths, and density contrasts, can be used to model the observed 40-mgal, short-wavelength, anomaly. However, a geologically reasonable causative body needs to be shallow, have limited lateral extent, and have a high-density contrast. The LaTraille and Hussong (1980) sonobuoy refraction profile passed over the southern flank of the gravity profile, and showed only a slight (<1-km) rise in the deep crustal layer (6.2 km/s).

We had hoped to place Site 458 on the crest of the gravity anomaly; however, with the reflection profiling equipment on the *Challenger*, we were unable to delineate enough sediments in the prime target area. The site was eventually located near 17°52'N and 146°56'E. This site had somewhat over 200 meters of recognizable sediment, which is enough to spud in securely the full bottom-hole assembly (essential for this deep-penetration objective), but it is about 8 km southeast of the center of the gravity anomaly. Our hope was that the cores from Site 458, if not of the material causing the anomaly, would be close enough to yield information on the cause of the anomaly.

The objectives of Site 458 were: (1) to determine the structure and origin of the outer fore-arc, particularly the acoustic basement material which may be related to the observed geophysical anomalies; (2) to determine the age and origin of the outer fore-arc which may have been part of the remnant Kyushu-Palau or West Mariana ridges that were drilled on DSDP Leg 59, or older marginal basin (Philippine Sea) oceanic crust, or uplifted Pacific oceanic plate material somehow transferred to the overriding fore-arc during the present phase of Mariana Trench subduction; (3) to relate the tectonics and geology of the outer fore-arc to the active volcanic arc, the frontal arc (Guam, Saipan, etc.) and the lower trench slope region (target areas SP-3C and SP-2B); and (4) to determine the physical properties and style of deformation of the outer fore-arc near Site 458, which is an area apparently dominated by tensional tectonics features (Hussong and Fryer, this volume; Mrozowski and Hayes, this volume), yet paradoxically is on the contact of two lithospheric plates which are converging at up to 10 cm/y. (Minster and Jordan, 1978).

OPERATIONS

The general location of Site 458 in the Mariana fore-arc region has long been of considerable geologic interest. However, the Active Margin Panel had given it relatively low immediate drilling priority, based on the possibility that this portion of the arc might have extra-thick sediments. Consequently, its exploration would have to await future IPOD full-riser drilling. However, interpretation of seismic, gravity, and magnetics profiles (Hussong and Fryer, this volume) and multi-channel seismic reflection data (Mrozowsky and Hayes, this volume) collected as part of the drill site selection surveys, suggested that parts of the fore-arc had shallow, high-velocity basement that was likely igneous material. Thus, by the beginning of Leg 60, a drill site in the middle of the fore-arc was regarded as technically possible and was considered an attractive alternative target.

After completion of the Mariana Trough series of holes and the failure of Site 457 on the axis of the volcanic arc, we found that we were well ahead of our drilling schedule, with only two top priority holes (Site Survey targets SP-3C and SP-2B) remaining. The last bit release sub-assembly had been lost at Hole 456A, so complete downhole logging was not possible until supplies (including a new bit release) were delivered to the *Challenger*. Rather than drill a highest priority site without downhole logging, we decided to drill at the alternative fore-arc site until delivery of the bit release sub-assembly.

After leaving Site 457, the *Challenger* proceeded directly to the center of the gravity high (17°54'N, 146°52'E) with all profiling gear (3.5-kHz and 12-kHz bathymetry, air-gun seismic reflection, and magnetometer) operational. We found that the sediments thinned very quickly as the gravity high was approached, and on the slight bathymetric irregularities near the center of the anomaly no recognizable sediments were observed. The profiling was, therefore, continued south and east until the seismic reflection records indicated a sediment thickness of over 200 meters. Although this site was on the periphery of the target gravity anomaly, after the drilling problems encountered on our previous sites we decided to go where the maximum opportunity for successful drilling (plenty of recognizable sediments) existed.

A 13.5-kHz double-life beacon was dropped at 0148 on 18 April 1978. A standard (120-m) bottom-hole assembly with a F93CK bit was rigged. The site was spudded at 0921 on 18 April at 17°51.85'N, 146°56.06'E in bottom 3449 meters below sea level. The coring summary and drilling rate are given in Table 1 and Figure 7.

For the first few cores recovery was good, but after Core 7 the sediments seemed to become more friable and recovery was very poor for the rest of the hole (21% for the site). Various combinations of bit weight, pumping pressure, and rotation rate were tried, but the recovery rate did not improve.

Heat flow measurements were made at 76.0 meters and 142.5 meters sub-bottom.

Igneous rocks were encountered at 256.5 meters (Core 29), and were cored for 209 meters.

After recovery of Core 38, the bit was temporarily plugged. Forty barrels of drilling mud were circulated through the hole in order to clean out the rubble that apparently caused the bit blockage. The hole remained fairly stable until Core 47, when additional torquing prompted the spotting of more mud. After recovery of Core 49, the drill pipe became stuck for over 30 minutes. We decided at this point that further drilling was not prudent. The bit could not be released, but we decided to attempt partial logging of the hole with the tools that could be run through the bit (temperature, gamma neutron, Francis resistivity). The flapper valve in the bit was held open with an empty inner barrel.

The bit was raised to 3569.5 meters below sea level (lifting everything except the 120 m of bottom-hole

Table 1. Coring Summary, Site 458.

Cores	Date (April 1978)	Time	Depth from	Depth below	Length Cored (m)	Recovery (m)	Recovery (%)
			Drill Floor (m)	Seafloor (m)			
			Top Bottom	Top Bottom			
1	18	1010	3459.0-3468.5	0.0-9.5	9.5	9.05	95.3
2	18	1130	3468.5-3478.0	9.5-19.0	9.5	8.92	93.9
3	18	1239	3478.0-3487.5	19.0-28.5	9.5	3.33	35.1
4	18	1355	3487.5-3497.0	28.5-38.0	9.5	2.75	29.0
5	18	1514	3497.0-3506.5	38.0-47.5	9.5	5.82	61.3
6	18	1627	3506.5-3516.0	47.5-57.0	9.5	4.80	51.1
7	18	1742	3516.0-3525.5	57.0-66.5	9.5	6.62	69.7
8	18	1857	3525.5-3535.0	66.5-76.0	9.5	0.35	3.6
9	18	2144	3535.0-3544.5	76.0-85.5	9.5	2.8	29.4
10	18	2249	3544.5-3554.0	85.5-95.0	9.5	0.03	0.3
11	19	0006	3554.0-3563.5	95.0-104.5	9.5	3.24	34.0
12	19	0113	3563.5-3573.0	104.5-114.0	9.5	0.03	0.3
13	19	0216	3573.0-3582.5	114.0-123.5	9.5	0.50	5.3
14	19	0325	3582.5-3592.0	123.5-133.0	9.5	0.28	3.0
15	19	0434	3592.0-3601.5	133.0-142.5	9.5	0.24	2.5
16	19	0734	3601.5-3611.0	142.5-152.0	9.5	3.43	36.1
17	19	0842	3611.0-3620.5	152.0-161.5	9.5	0.21	2.2
18	19	0958	3620.5-3630.0	161.5-171.0	9.5	0	0
19	19	1105	3630.0-3639.5	171.0-180.5	9.5	2.10	22.1
20	19	1212	3639.5-3649.0	180.5-190.0	9.5	0	0
21	19	1330	3649.0-3658.5	190.0-199.5	9.5	0.05	0.5
22	19	1441	3658.5-3668.0	199.5-209.0	9.5	0.30	3.0
23	19	1605	3668.0-3677.5	209.0-218.5	9.5	0	0
24	19	1728	3677.5-3687.0	218.5-228.0	9.5	1.12	11.8
25	19	1907	3687.0-3696.5	228.0-237.5	9.5	3.23	34.0
26	19	2115	3696.5-3706.0	237.5-247.0	9.5	0.67	7.0
27	19	2307	3706.0-3715.5	247.0-256.5	9.5	2.17	22.8
28	20	0051	3715.5-3725.0	256.5-266.0	9.5	0.81	8.5
29	20	0221	3725.0-3734.5	266.0-275.5	9.5	2.53	26.6
30	20	0355	3734.5-3744.0	275.5-285.0	9.5	1.28	13.47
31	20	0528	3744.0-3753.5	285.0-294.5	9.5	0.76	8.0
32	20	0709	3753.5-3763.0	294.5-304.0	9.5	3.20	33.7
33	20	0915	3763.0-3772.5	304.0-313.5	9.5	2.30	24.2
34	20	1121	3772.5-3782.0	313.5-323.0	9.5	1.50	15.8
35	20	1321	3782.0-3791.5	323.0-332.5	9.5	2.40	25.3
36	20	1535	3791.5-3801.0	332.5-342.0	9.5	1.75	18.4
37	20	1706	3801.0-3810.5	342.0-351.5	9.5	1.20	12.6
38	20	1851	3810.5-3820.0	351.5-361.0	9.5	0.49	5.2
39	20	2125	3820.0-3829.5	361.0-370.5	9.5	2.35	24.7
40	20	2324	3829.5-3839.0	370.5-380.0	9.5	2.38	25.1
41	21	0057	3839.0-3848.5	380.0-389.5	9.5	2.49	26.2
42	21	0240	3848.5-3858.0	389.5-399.0	9.5	1.13	11.9
43	21	0410	3858.0-3867.5	399.0-408.5	9.5	1.50	15.8
44	21	0543	3867.5-3877.0	408.5-418.0	9.5	1.43	15.0
45	21	0733	3877.0-3886.5	418.0-427.5	9.5	1.70	17.9
46	21	0910	3886.5-3896.0	427.5-437.0	9.5	0.74	7.8
47	21	1106	3896.0-3905.5	437.0-446.5	9.5	1.70	17.9
48	21	1327	3905.5-3915.0	446.5-456.0	9.5	1.25	13.2
49	21	1555	3915.0-3924.5	456.0-465.5	9.5	0.90	9.5
Total					465.5	97.83	21.0

assembly out of the hole), and the temperature log was rigged. Unfortunately, the T-log tool would not go past 3566 meters of wire-out, indicating that it was blocked at the top of the inner barrel. The same results occurred with the gamma neutron log. It was then apparent that the hole could not be entered through the bit, and therefore could not be logged, so the drill string was pulled and secured aboard. The bit and inner barrel showed no signs of abnormality on deck, so we do not know the reason for the failure of the logging effort.

The *Challenger* made two more passes over the Site 458 beacon with the regular geophysical profiling equipment, and then departed for Site 459 at 1300 on 22 April 1978.

Within a few hours after our completion of Site 458 we received a radio message indicating that the supply ship, which was supposed to bring us a bit release and other supplies prior to logging at Site 459, had engine failure. At that time we decided to change course and headed directly for Saipan to pick up the necessary equipment.

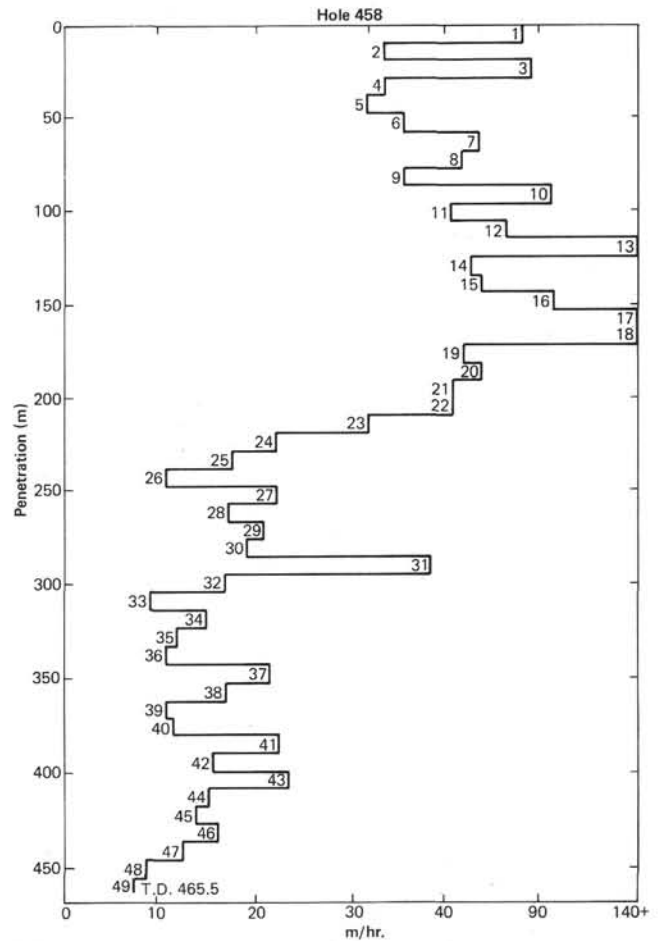


Figure 7. Coring rate (m/hr.) versus depth below seafloor, Site 458.

SEDIMENT LITHOLOGY

At Site 458, 256.5 meters of sediment was penetrated before reaching basalts. Four units can be distinguished, as shown in Figure 8.

Unit I: 0 m to 28.5 meters (Cores 1-3); Pleistocene to late Pliocene. Siliceous-nannofossil-foraminifer-vitric mud; siliceous-foraminifer nannofossil-ooze and silty-vitric ash.

The lithology of this unit is variable, but the sediments are characterized by an abundance of volcanic ash (glass and feldspar) and biogenic components (both siliceous and calcareous). Foraminifers (1/2-1%) are visible to the unaided eye in Core 1 to Core 2, Sections 1 through 3.

Unit II: 28.5 m to 95.0 meters (Cores 4-10); late Pliocene to middle Miocene. Nannofossil ooze, vitric-nannofossil ooze, siliceous-nannofossil ooze with thin beds of silty to sandy vitric ash.

The lithology is more uniform in this unit than in Unit I. Volcanic ash is richer in Core 5, Section 4 to Core 7, Section 2. Radiolarians are richer in Core 6, Section 6 to Core 7.

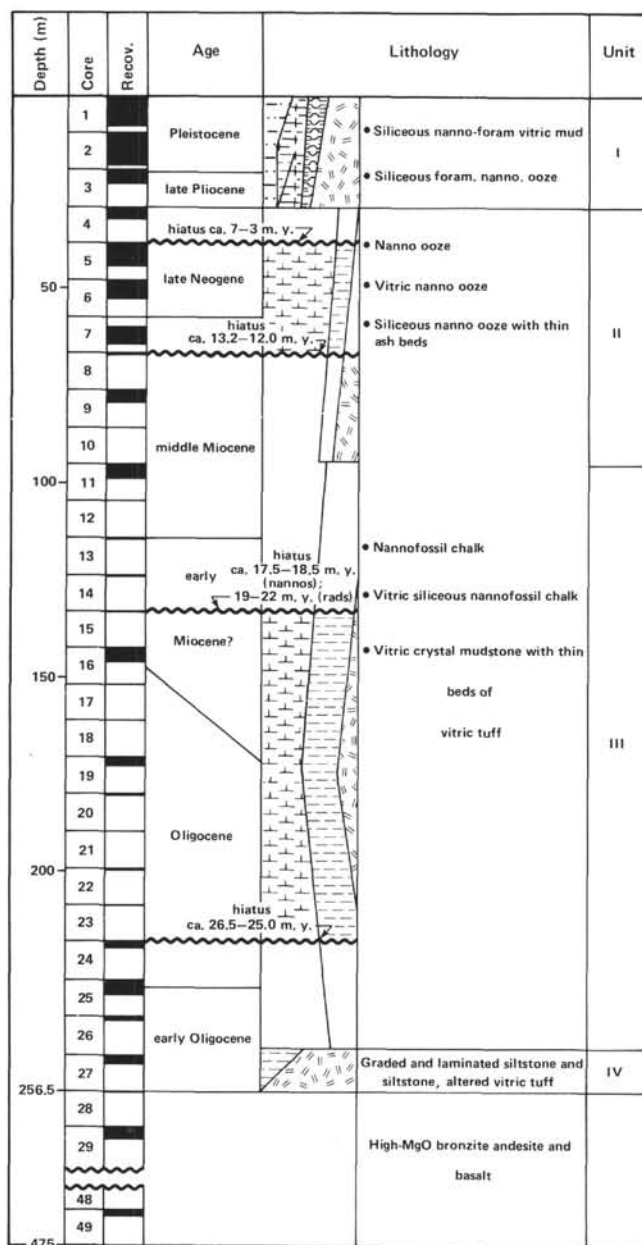


Figure 8. Sediment lithology, age, recovery per core, and lithologic units versus depth, Site 458.

Several minor hiatuses exist in Units II between Cores 4, CC and 5, Section 1 (some 4 m.y. between ca. 3 and 7 m.y. B.P.) and between Core 7, Section 4, and Core 7, CC (some 1.2 m.y. between 12 and 13.2 m.y. B.P.). Nannofossils give clear evidence for the hiatuses, since full zones and subzones are absent. Radiolarian dates are consistent with the absence of these intervals.

Unit III: 95 m to 247 meters (Cores 11-26); middle Miocene to early Oligocene. Nannofossil chalk, vitric-siliceous-nannofossil chalk, vitric-crystal mudstone with thin silty to sandy vitric tuff.

The lithology is even more uniform in this unit than in Unit II. Sudden increases in lithification occur at the top of Cores 11 and 16. Nannofossil chalk in Cores 13

through 15 is softer than chalks in Core 11. Below this, burrows occur in both chalk and mudstone. Volcanic ash is less abundant than in other units. It is particularly low in Cores 11 through 14 (12?).

In the catcher of Core 12, several lithified sedimentary and igneous pebbles were recovered. One of these, a coarse sandstone, yielded nannofossils of early Oligocene age.

An hiatus exists between Cores 14 and 15, although the age and duration of this period of non-deposition or erosion are uncertain. Nannofossil identifications suggest the hiatus occurred at about 17 m.y. B.P., whereas radiolarian assemblages suggest the hiatus lasted from ca. 19 to ca. 22 m.y. B.P. A second, better defined, hiatus exists between Core 23, CC and 24, Section 1. The length of this hiatus is some 1.5 m.y. from ca. 25 to ca. 26.5 m.y. B.P.

Unit IV: 247 m to 256.5 meters (Core 27); early Oligocene. Laminated and graded vitric siltstone, sandstone (greenish), and altered vitric ash (pale green to moderate red) with extensive black spots (Mn?). This unit is characterized by graded vitric siltstone and sandstone with abundant volcanic ash (~90%). Within the unit, however, the ash content diminishes greatly upward into the ash-poor Unit III.

A fine vitric sandstone from Section 1, 65-75 cm, was cut by a 1-cm-thick vein dipping 80°. The talcose vein material has slickensides with horizontal striations.

BIOSTRATIGRAPHY

Summary

Diverse Quaternary to early Oligocene calcareous nannoplankton and radiolarian assemblages occur throughout the sedimentary interval (Cores 1-27) overlying the igneous rocks at Site 458.

The absence of several nannoplankton and radiolarian zones in the early Pliocene and late Miocene interval indicates a major hiatus. Nannoplankton evidence suggests a minimum gap of about 4.0 m.y. between Cores 4 and 5.

Three other interruptions in the continuity of sedimentation occur in the middle Miocene, early Miocene, and Oligocene. Nannoplankton evidence indicates that an hiatus of 1.2 m.y. occurs between Samples 7-4, 90-91 cm and 7, CC in the middle Miocene. Another hiatus of undetermined length occurs in the interval between Samples 14, CC and 15, CC in the early Miocene. Finally, the equivalent of 1.5 m.y. is missing between Samples 23, CC and 24-1, 45-46 cm in the late Oligocene.

Redeposition of considerably older fossil assemblages occurred at two different stratigraphic levels. A limestone pebble of Oligocene age was found associated with late early Miocene sediment of Core 12. Early Eocene radiolarians and nannoplankton in the Oligocene sediment of Section 1 of Core 27 suggest a nearby outcrop of Eocene, when sediments began to accumulate over the igneous rocks.

The sparse occurrence of foraminifers in all samples throughout the sedimentary sequence may indicate deposition near their compensation surface, which is nor-

mally shallower than the compensation surface for calcareous nannoplankton. On the other hand, abundant calcareous nannoplankton—resulting in nannoplankton chalks and oozes—clearly indicate that the site was well above the nannoplankton compensation surface throughout its sedimentary history.

Nannoplankton

In addition to examining a complete suite of samples from the sedimentary sequence overlying the igneous basement, fine-grained rock material intermixed with basalts was examined from Cores 28, 29, 30, 31, 35, 40, and 48.

Nannoplankton assemblages observed throughout the sedimentary interval in Hole 458 show good species diversity and contain age-diagnostic forms.

A nearly continuous sequence of zones and subzones from Holocene through late Pleistocene through late Pliocene can be recognized (Samples 1-1, 90-91 cm through 4,CC). Only the *Emiliana annula* Subzone of the *Crenolithus daronicoides* Zone and the *Discoaster surculus* Subzone of the *D. brouweri* Zone cannot be identified.

Samples from Core 5 and Section 1 of Core 6 can be assigned to the *Discoaster neorectus* Subzone of the late Miocene *D. neohamatus* Zone. This absence of early Pliocene and late Miocene nannoplankton zones is the basis for recognizing an hiatus of 4.0 m.y. (3.0 m.y. B.P. to 7.0 m.y. B.P.) between Samples 4,CC and 5-1, 55-56 cm. The remainder of Core 6 can be assigned to the *Discoaster bellus* Subzone of the *D. neohamatus* Zone.

Cores 7 through 11 are of middle Miocene age with all of the nannoplankton zones and subzones present, except the *Helicosphaera carteri* Subzone of the *Discoaster hamatus* Zone and the *Catinaster coalitus* Zone. This hiatus of 1.2 m.y. (12.0 m.y. B.P. to 13.2 m.y. B.P.) is recognized between Samples 7-4, 90-91 cm and 7,CC.

Samples 12,CC through 14,CC are assigned to the early Miocene *Helicosphaera ampliaperta* Zone, although the name species is not present. The absence of *H. ampliaperta* from this zone was reported by Ellis (1975) at DSDP Site 292 (Leg 31) in the western Philippine Sea. Although the *H. ampliaperta* Zone was not recognized at that time, re-evaluation of the data now permits identification of the zone at Site 292. It has been suggested that *H. ampliaperta* is a colder-water species, thus accounting for its absence at Sites 292 and 458. In support of this theory, the presence of this species was noted by Ellis at Site 296 at the extreme northern end of the Philippine Sea.

Sample 15,CC is assigned to the *Sphenolithus belemnoides* Zone. The species *S. belemnoides* and *Triquetrorhabdulus milowii* have their last occurrence above the first occurrence of *S. heteromorphus* in normal low-latitude deep-sea sediment sequences. The absence of this occurrence overlap in Hole 458 suggests a period of nondeposition or sediment removal between Samples 14,CC and 15,CC.

The *Discoaster druggii* Subzone of the *Triquetrorhabdulus carinatus* Zone is determined for Samples 16-1, 42-43 cm through 19-1, 67-68 cm. The other two subzones of this zone cannot be identified with any confidence; however, the last occurrence of an abundance acme of *Cyclicargolithus abisectus*, which defines the top of the *C. abisectus* Subzone, is seen in Sample 17,CC. Interpretation of the significance of this unexpected overlap of defining criteria, together with the apparent absence of the intervening *Discoaster deflandrei* Subzone, is complicated by the reduced number of samples (there was no recovery in Core 18) through the interval. As a result of this conflicting evidence, the Miocene/Oligocene boundary (23 m.y.), which is drawn at the top of the *Cyclicargolithus abisectus* Subzone, is placed between Samples 16,CC and 19,CC. Samples 22,CC and 23,CC are clearly in the late Oligocene *Sphenolithus ciperoensis* Zone.

The lower subzone of the *Sphenolithus ciperoensis* Zone, the *Cyclicargolithus floridanus* Subzone, is defined as that interval where *S. ciperoensis* and *S. distentus* occur together. Since these two species have this occurrence relationship in the western and northern Philippine Sea at Sites 292 and 296 (Ellis, 1975), the absence of the *C. floridanus* Subzone in these samples may indicate an hiatus of about 1.5 m.y. in Hole 458 between Samples 23,CC and 24-1, 45-46 cm.

The late Oligocene *Sphenolithus distentus* Zone is recognized in samples from Core 24. Cores 25, 26, and 27 contain an assemblage that is referred to as the *S. predistentus* Zone.

Several bits of fine-grained rock material, occurring in conjunction with the basalts, were examined from Cores 28 through 48 in an attempt to date the various pillow lavas. Two sparse occurrences (Sample 29-1, Piece 1 and Section 40-1) are interpreted as contamination from uphole.

The core catcher samples from Core 12 contain some limestone pebbles in addition to the fine-grained, softer sediments. Nannoplankton recovered from these pebbles can be referred to the late Oligocene *Sphenolithus distentus* Zone or early *S. ciperoensis* Zone.

Radiolarians

Radiolarians occur throughout Hole 458, with only a few, sporadic barren samples. The sequence ranges from Quaternary back through the early Oligocene. Most of the zones can be recognized in sequence, except where there are hiatuses, but scarcity of several zone-defining species hinders exact placement of boundaries.

The Quaternary is represented in Core 1, where the *Collosphaera tuberosa* Zone is recognizable. Core 2 is also Quaternary, but zones cannot be distinguished.

Core 3 lacks species that are clearly definitive of either Quaternary or Pliocene, but is tentatively considered Pliocene. Core 4 contains no age-diagnostic species.

The late Miocene *Ommatartus penultimus* Zone is tentatively recognized in the upper part of Core 5. Since the next higher (also late Miocene) zone was not recog-

nized, an hiatus spanning latest Miocene and possibly early Pliocene occurs between Cores 3 and 5.

The *Ommatartus antepenultimus* Zone is recognizable in the bottom of Core 5 and upper part of Core 6. The bottom of Core 6 and upper part of Core 7 are tentatively identified with the middle Miocene *Cannartus petterssoni* Zone. The *Dorcadospyrus alata* Zone is tentatively recognized from the bottom part of Core 7 through Core 10.

The early Miocene *Calocycletta costata* Zone can be recognized in Cores 11 and 12. Cores 13 and 14 belong to the next lower *Stichocorys wolffii* Zone. An hiatus separates that zone from the *Cyrtocapsella tetrapera* Zone in Core 15, with the *Stichocorys delmontensis* Zone missing. The *C. tetrapera* Zone continues through Core 19.

No zones can be recognized in Cores 21 and 22, which are either early Miocene or late Oligocene in age. Between Cores 22 and 24, the transition from the late Oligocene *Dorcadospyrus atechus* Zone, to the early Oligocene *Theocyrtis tuberosa* Zone takes place.

Sample 27-1, 24-26 cm, contains a well-preserved assemblage of radiolarians belonging to the early Eocene *Buryella clinata* Zone. These specimens are apparently reworked into sediments dated as Oligocene on the basis of calcareous nannoplankton.

Foraminifers (V. A. Krashennikov)

At Site 458, impoverished assemblages of foraminifers range in age from Quaternary through Pliocene and Miocene to Oligocene. Diversity and preservation permit only isolated age diagnoses.

The late Quaternary *Globigerina calida calida* Subzone can be recognized in Samples 1-1, 50-52 cm through 1-5, 50-52 cm. The early Quaternary, based on the presence of *Globorotalia truncatulinoides* and *Globorotalia tosaensis*, is recognized in Samples 2-2, 50-52 cm through 2-6, 50-52 cm.

Foraminifers are rare in Samples 3-1, 50-52 cm through 4-1, 50-52 cm, permitting only an undifferentiated Quaternary-Pliocene assignment.

The early Pliocene *Globorotalia margaritae evoluta* Zone is represented in Samples 5-1, 50-52 cm through 5-3, 50-52 cm. In Samples 5-4, 50-52 cm through 7-4, 50-52 cm, foraminifers are poor and either early Pliocene or late Miocene (with *Globigerina nepenthes*).

The late Miocene is recognized in Core 9 (Samples 9-1, 52-54 cm and 9-2, 50-52 cm), where *Sphaeroidinellopsis subdehiscens* occurs without Pliocene species.

The middle Miocene is recognized in Sample 11-1, 50-52 cm, but no zones can be diagnosed. Similarly, poor foraminifers in Samples 14, CC through 19-2, 32-35 cm indicate undifferentiated early Miocene.

The Miocene/Oligocene boundary seems to be near Sample 21-5, 5-7 cm. The undifferentiated Oligocene is recognizable on the basis of poor assemblages in Samples 22, CC through 25-1, 53-55 cm. The Oligocene *Globorotalia opima* Zone is represented in Sample 25-2, 44-46 cm.

SEDIMENT ACCUMULATION RATES

Paleontological data provide two sets of relative ages; one from calcareous nannoplankton, the other from radiolarians. They are plotted on an age-sediment accumulation diagram (Fig. 9) based on the zonation scheme related to absolute time of Figure 8 in the introductory chapter of this volume. The sediment accumulation has been calculated as outlined for Site 453. Radiolarian data are plotted only when they provide ages different from those given by nannoplankton.

Generally, the two sets of data show good agreement. However, in samples from Cores 13 through 16, the ages range somewhat differently. In these samples, the age ranges determined from the two sources show disagreement of over 5 m.y. for Core 15 and over 1 m.y. for Cores 13, 14, and 16. The radiolarian age is generally greater and is more irregular. This may reflect the imperfection in the dating of these biostratigraphic zonations and/or poorer control of radiolarian zonations.

Accumulation rates at Hole 458 have been very low, averaging 0.76 kg/cm²/m.y., throughout the history of sediment deposition at the site. The sediment accumulation curve from nannoplankton data falls into three major segments, each bounded by hiatuses, as indicated in Table 2. Fluctuations in the accumulation rate appear to have occurred within these segments.

Within the oldest segment, a reliable rate calculation is prevented by the very poor recovery. The initial rate of accumulation was 0.5 kg/cm²/m.y. until 26 m.y. B.P., after which the rate increased. Two hiatuses were suggested in this segment: the older between Cores 23 and 24, and the younger between Cores 14 and 15. The older hiatus lasted for about 1 m.y., and occurs after the initial slower sedimentation (Fig. 9). The younger hiatus is more doubtful. The accumulation rate curve for the younger half of the oldest segment, based on radiolarian age determinations, diverges markedly from the nannoplankton curve. It indicates very rapid sedimentation during the short *Cyrtocapsella tetraperta* Zone (Cores 15 through 19), succeeded by a 3-m.y. hiatus. Reworking of radiolarians could explain the difference between the curves derived from the two fossil groups and the presence of an apparent hiatus of 3 m.y. in one of them.

The accumulation of sediments is once again low in the second segment (7-12 m.y.). This interval probably

Table 2. Sediment accumulation rates, Hole 458.

Core No.	Duration (m.y.B.P.)	Accumulation Rate (kg/cm ² /m.y.)
0-4	0-3	1.1
Hiatus	3-7	
5-7(5)	7-12	0.5
Hiatus	12-13	
7(5)-27	13-25	1.8

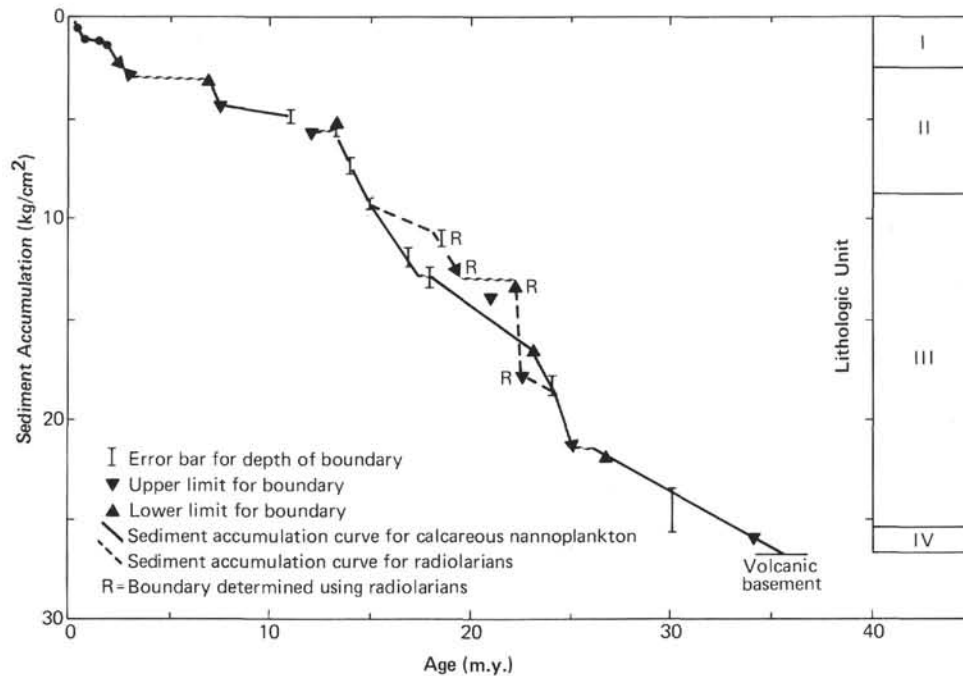


Figure 9. Sediment accumulation (kg/cm^2) versus age, Site 458. Separate curves are plotted for calcareous nannoplankton and radiolarians.

corresponds to the last stage of volcanism on the West Mariana Ridge prior to the formation of the Mariana Trough.

The faster accumulation of sediment in the most recent segment (3 m.y. to the present) may be the result of the volcanic activity on the present arc, with the preceding hiatus resulting from tectonic activity prior and subsequent to rifting of the arc.

STRATIGRAPHIC SYNTHESIS

The sedimentary sequence drilled at Site 458 has several distinctive features when compared with (1) the sediment found in the Mariana Trough (Sites 453 through 456) and (2) the sediments recovered at Site 452, on the Pacific plate, just eastward of the Mariana Trench.

These characteristics are:

- 1) considerable development of carbonate (up to 91% calcareous ooze and chalk).
- 2) the abundance of biogenic components, e.g., nanofossils all through the sequence. Diatoms and radiolarians occur more frequently in the seven uppermost cores. Foraminifers are abundant only in the first three cores (0–28.5 m).
- 3) the presence of strongly altered vitric tuff in the early Oligocene between the nanofossil chalk and the basalt. They are laminated, sometimes graded sandstone and siltstone (turbidites), mainly green, with over 70 percent of altered volcanic glass.
- 4) the occurrence of abundant reworked material: early Oligocene nanofossil chalk, igneous rocks, vesicular basalts, coarse sandstones, in the middle Miocene;

early Eocene radiolarian-bearing sediments in early Oligocene sandstones.

5) the presence of volcanic glasses and ash layers throughout the sequence. In general, however, after the early Oligocene vitric tuff in the basal sediment (Core 27), there is a sharp decrease in the amount of volcanogenic material in the cores, quickly reaching a minimum in the nanofossil chinks in Core 25 (still early Oligocene). The volcanogenic component remains fairly low, but slowly increases until late Miocene, when it jumps to the high proportion predominant through to the present.

The basement rocks at Site 458 are fractured and slickensided (Igneous Rocks section, this chapter). The scale of the shearing and faulting is difficult to determine, and we cannot say if this deformation records tectonic processes predating the oldest sediments (early Oligocene).

The basal sediment (Core 27) is a laminated, but rarely graded, green sandstone and siltstone consisting mainly of strongly altered volcanic glass (vitric tuff). The reworked volcanic material and some volcanic activity thus predate the sediment itself, which is early Oligocene in age (*S. predistentus* Zone).

The sedimentation then became dominantly biogenic (calcareous) in Unit III. Volcaniclastic components decrease markedly to a minimum fraction in Core 25 (early to late Oligocene). This trend could indicate a minimum in arc volcanic activity at this time (~30 m.y. B.P.). At no time do we observe a complete absence of ash in the cores. By late Oligocene (Cores 21 and 22), volcanic glass and feldspars are more abundant, giving

silty and sandy ash layers or vitric debris in the nanofossil chalk. In Unit III, reworked older sediments, as well as igneous pebbles (Core 12), show that some source regions were eroded during Oligocene and early and middle Miocene times.

The hiatuses also give evidence for instability in the sedimentary process (erosional and/or non-depositional conditions).

The uppermost units consist of Plio-Pleistocene nanofossil vitric mud and nanofossil vitric ooze, with siliceous-nanofossil ooze represented mainly in the top of Unit I (Cores 1 and 2), and the middle of Unit II (Cores 7 and 8).

Site 458 was clearly above the carbonate compensation depth between the early Oligocene and the Pleistocene. However, the scarcity of foraminifers would indicate, in some cases, depths below the compensation surface for foraminifers.

The stratigraphic sequence at Site 458 is unlike that of nearby off-ridge drill sites (Site 452 on the Pacific plate, Sites 453 through 456 in Mariana Trough, and Sites 449 and 450 in the Parece Vela Basin). It is interesting, however, to consider the relative location of Site 458 in the past, backtracking this site (after Karig, 1971) to its location before the opening of the Mariana Trough and that of the Parece Vela Basin (Fig. 1). During the late Miocene, Site 458 was in the vicinity of Site 451 (West Mariana Ridge), and in the early Oligocene it was in the same area as Site 448 (Palau-Kyushu Ridge). Thus the pre-Pliocene column at Sites 458 and 451, and the pre-Miocene column at Sites 458, 451, and 448 should show affinities (or at least no disagreement). The comparisons are consistent with this simple evolutionary model.

The stratigraphic column at Site 458 also shows similarities with DSDP Sites 292 (Benham Rise, Leg 31) and 445 (Daito Ridge, Leg 58), both located in the West Philippine Sea. Facies from the same age are comparable; carbonates are well developed, reworked materials are frequent in all three sites. Hiatuses are present (upper Miocene at Sites 458 and 292; Oligocene at Site 445). Nanofossil assemblages are similar in Sites 458 and 292.

The main environmental conditions on all the "ridges" in the Philippine Sea remained more or less the same during Cenozoic time. There was a high biogenic contribution, mainly of nanofossils, permitting the development of thick nanofossil chinks and oozes on the ridges. Erosional processes, or other factors preventing sediment deposition, may have been tectonically controlled in the area by factors such as rifting, because hiatuses often correlate in the columns.

For these sites with high biogenic chalk and ooze components, the biostratigraphy suggests a previous location not far from the equatorial zone of high productivity. This hypothesis is consistent with the paleomagnetic analysis made during this leg (see Bleil, this

volume). The latter indicates that the Mariana fore-arc at 18°N has migrated from an almost equatorial latitude to its present position over the past 35 m.y.

INTERSTITIAL WATER GEOCHEMISTRY

Six samples for interstitial water chemistry were taken from sediments at Site 458. The data are given in Gieskes and Johnson (this volume). Briefly, a marked increase in Ca^{2+} and decrease in Mg^{2+} occur with depth, probably a consequence of reaction between pore fluids and volcanic glass in the sediments, or with basement rocks. The lowest sample appears to have been contaminated with fresh water during core splitting.

PHYSICAL PROPERTIES

Compressional wave velocity, wet-bulk density, salt-corrected water content, porosity, acoustic impedance, and thermal conductivity were determined for samples recovered from Site 458. Sonic velocities were measured for the vertical direction in the Hamilton Frame. The densities of the same samples were determined by 2-minute GRAPE counts. A proportion of these samples were then subjected to gravimetric determination of density, porosity, and water content. The measurements are tabulated in Table 3.

Density and Sonic Velocity

Density and sonic velocity are plotted against depth in Figure 10. Down to about 140 meters sub-bottom, the sediments were unlithified. There followed two cores (Cores 16 and 17) of lithified sediments, principally mudstones and chalk, from which samples had to be sawn. These samples produced the higher velocities near 150 meters on the velocity-depth plot. The nanofossil chalk recovered in Core 19 was less lithified, but from this level the chinks became more lithified, with both velocity and density gradually increasing with depth. However, velocities as high as those near a 150-meter depth (~2 km/s) were not reached again until very close to the base of the sediment, at about 255 meters.

In contrast to the velocity-depth plot, that of density against depth (Fig. 10) shows only a gradual increase of density down the sedimentary column. The pronounced increase in velocity near 150 meters sub-bottom is not reflected in the density profile.

The igneous rocks sampled below 255 meters were all altered to some degree. Some had extremely low velocities and were so soft that they could be scratched with a fingernail or plastic knife. The sonic velocities of the igneous rocks are plotted against their densities in Figure 11. The two correlate extremely well.

Samples from Cores 32 to 34 (294.5–323.0 m sub-bottom) were some of the more massive high-MgO, bronzite andesites (see Igneous Rocks, this chapter). These rocks appear to be the least altered of the rocks recovered, and plot at the higher end of the velocity and density scale.

Table 3. Velocity-density measurements, Site 458.

Sample (interval in cm)	Depth (m)	Sound Velocity (km/s)	GRAPE ^a Wet-Bulk Density (g/cm ³)	Wet Water Content ^b (%)	Porosity ^c (%)	Wet- Bulk Density ^d (g/cm ³)	Acoustic Impedance ^e (g/cm ² s × 10 ²)	Rock Type
1-2, 22-24	1.72	1.54		44.1	68.1	1.58	2.43	Mud
1-4, 103-105	5.53	1.53	1.64				2.51	Mud
2-1, 115-117	10.65	1.55	1.62				2.51	Mud
2-2, 83-85	11.83	1.56	1.64	42.0	66.1	1.61	2.51	Firm Mud
2-3, 63-65	13.13	1.56	1.58				2.46	Firm Mud
2-5, 27-29	15.77	1.55	1.65				2.56	Mud
3-1, 64-66	19.64	1.55	1.55	46.5	70.0	1.54	2.39	Firm Mud
3-2, 64-66	21.14	1.55	1.56	46.4	69.6	1.53	2.37	Firm Mud
4-1, 122-124	29.72	1.53	1.58	48.6	71.5	1.51	2.31	Firm Mud
4-2, 15-17	30.15	1.55	1.66	40.0	64.1	1.64	2.54	Firm Mud
5-1, 63-65	38.63	1.53	1.63				2.49	Ooze
5-2, 67-69	40.17	1.56	1.63	44.3	67.6	1.56	2.43	Ooze
5-3, 44-46	41.44	1.55	1.63				2.53	Firm Ooze
5-4, 48-50	42.98	1.56	1.52				2.32	Firm Ooze
6-1, 36-38	47.86	1.56		44.9	68.0	1.55	2.42	Stiff Ooze
6-2, 46-48	49.46	1.55	1.65	43.2	66.7	1.58	2.45	Mud
6-3, 127-129	51.77	1.58	1.65				2.61	Firm Mud
7-1, 92-94	57.92	1.59	1.66	36.7	60.6	1.69	2.69	Firm Mud
7-3, 33-35	60.33	1.60	1.56				2.50	Firm Mud
7-4, 121-123	62.71	1.56	1.66	41.3	65.2	1.62	2.53	Firm Mud
9-2, 25-27	77.75	1.58	1.63	42.0	64.9	1.58	2.50	Firm Mud
11-1, 108-110	96.08	1.57	1.56	43.8	67.1	1.57	2.46	Firm Ooze
11-2, 102-104	97.52	1.58	1.64				2.59	Firm Ooze
13-1, 30-32	114.30	1.60	1.64	40.4	63.9	1.62	2.59	Firm Mud
16-1, 17-19	142.67	2.12	1.80	31.7	55.2	1.79	3.79	Mudstone
16-2, 41-43	144.41	1.86	1.61				2.99	Mudstone
17-1, 9-14	152.09	2.00	1.80				3.60	Siltstone
19-1, 51-54	171.51	1.63	1.82				2.97	Nanno Chalk ^e
19-2, 22-25	172.72	1.61	1.72	34.6	57.4	1.70	2.74	Nanno Chalk ^e
24-1, 4-6	218.54	1.62	1.82	32.1	55.2	1.76	2.85	Nanno Chalk
25-1, 68-70	228.68	1.66	1.84	32.4	55.4	1.76	2.92	Nanno Chalk
25,CC, 14-17	230.99	1.76	1.92				3.38	Nanno Chalk
26-1, 34-36	237.84	1.73	1.92	27.2	49.2	1.85	3.20	Nanno Chalk
27-1, 56-58	247.56	1.91	1.64	40.5	63.7	1.61	3.08	Calc. Tuff
27-2, 26-28	248.76	2.52	1.81	26.2	48.2	1.88	4.74	Sandstone
28-1, 110-112	257.60	3.79	2.32	15.6	34.4	2.26	8.57	Altered Basalt
29-1, 93-95	266.93	3.17	2.17	16.6	35.5	2.19	6.94	Alt. Basalt
29-2, 82-84	268.32	3.25	2.14	19.7	40.3	2.09	6.79	Alt. Basalt
29-3, 60-62	269.60	3.15	1.97	18.4	38.6	2.15	6.77	Alt. Basalt
30-1, 110-112	276.60	3.21	2.27	16.1	34.9	2.23	7.16	Alt. Basalt
30-2, 71-73	277.71	3.16	2.15	19.9	40.0	2.06	6.51	Alt. Basalt
31-1, 125-128	286.25	3.84	2.48	9.9	23.4	2.43	9.33	Alt. Basalt
32-1, 48-50	294.98	3.98	2.45	9.0	21.4	2.44	9.71	Ves. Basalt
32-3, 112-117	298.62	4.36	2.56				11.2	Basalt
33-1, 112-115	305.12	4.71	2.68	5.1	13.0	2.63	12.4	Basalt
33-2, 63-68	306.13	4.25	2.56				10.9	Basalt
34-1, 113-118	314.63	4.23	2.53				10.7	Veined Basalt
35-1, 100-102	324.00	3.84	2.42				9.29	Ves. Basalt
35-2, 43-45	324.93	3.36	2.23	17.4	36.8	2.17	7.29	Basalt
36-1, 58-60	333.08	3.26	2.33	15.3	33.3	2.23	7.27	Basalt
37-1, 72-76	342.72	3.80	2.40				9.12	Alt. Basalt
38-1, 49-53	351.99	3.85	2.42				9.32	Ves. Basalt
39-1, 102-108	362.02	3.24	2.21				7.16	Basalt
39-2, 60-62	363.10	3.56	2.33	13.8	30.7	2.28	8.12	Basalt
40-1, 79-85	371.29	3.01	2.20				6.62	Basalt
41-1, 122-124	381.33	2.83	2.13	18.1	37.5	2.13	6.03	Basalt
42-1, 133-136	390.83	5.08	2.52				12.8	Ves. Basalt
43-1, 146-150	400.46	2.91	2.21				6.43	Alt. Basalt
44-1, 71-73	409.21	3.27	2.23	17.3	37.1	2.19	7.16	Alt. Basalt
45-2, 70-74	420.20	2.58	2.09				5.39	Alt. Basalt
46-1, 85-87	428.35	3.19	2.21	16.4	35.4	2.21	7.05	Alt. Basalt
47-1, 81-83	437.81	2.87	2.30	14.5	32.0	2.26	6.49	Alt. Basalt
48-1, 39-41	446.89	3.05	2.28	14.8	33.1	2.29	6.98	Alt. Basalt
49-1, 135-137	457.35	3.20	2.28	14.8	32.4	2.24	7.17	Alt. Basalt

^a a = From 2-min. counts.

^b Salt-corrected.

^c c = Porosity = (Salt-corrected wet water content) × [Wet-bulk density (gravimetric)]/1.025.

^d Gravimetric method.

^e Unlithified.

The variation of velocity and density with depth for the igneous rocks is also shown in Figure 10. The general decrease of both velocity and density with depth apparently reflects the greater degree of alteration of the deeper flows.

Thermal Conductivity

The thermal conductivities of core samples from Site 458 were measured, and the profile of thermal conductivity of the upper oceanic crust was constructed to the sub-bottom depth of 460 meters. The results of this

study are reported by Horai, this volume. In summary, Horai found that in the sediments there is a rate of increase of thermal conductivity with depth of (0.23 mcal/cm s °C)/100 meters. In the basement igneous rocks, Horai (this volume) also finds a strong correlation of thermal conductivity with lithology of the strata.

HEAT FLOW

From two bottom-hole sediment temperature measurements (at sub-bottom depths of 76 m and 142.5 m), heat flow at this site is estimated to be a 0.6 HFU. This

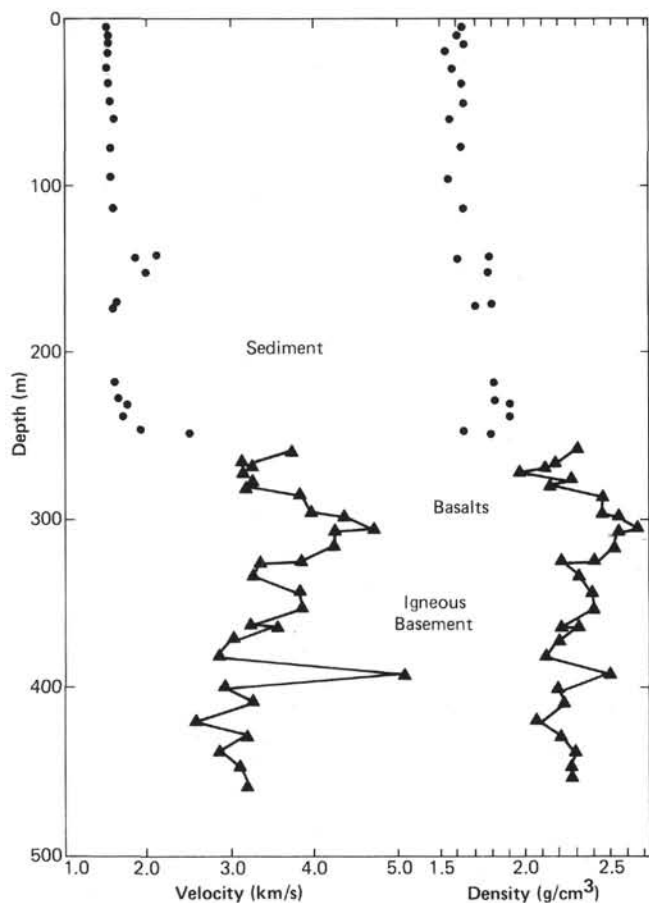


Figure 10. Sonic velocity (km/s) and density (g/cm^3) versus depth below seafloor for sediments (dots) and igneous rocks (open triangles), Site 458.

value is not highly reliable because of uncertainty in the interpretation of observed temperatures. See Uyeda and Horai (this volume).

IGNEOUS ROCKS

Lithology

The total penetration of igneous basement in Hole 458 (209 m) exceeds that of any other hole drilled in a frontal-arc province. However, recovery of this material in individual cores was low to moderate (5.3–33.7%).

The sequence of rocks recovered consists of alternating pillows and flows, some of which are highly fractured and altered. There are two principal rock types, defined by petrography and chemistry, comprising four distinct chemical types (based primarily on Wood et al., this volume). The types are designated A, for andesite, and B, for basalt (Fig. 12), as follows:

- A₁: 256.5 to 380 meters below the seafloor, Cores 28–40: pillows and flows of high-MgO, bronzite-bearing andesite related to the boninite suite;
- B₁: 380 to 389.5 meters below the seafloor, Core 41: highly fractured and altered tholeiitic basalts resembling island-arc tholeiites;
- A₂: 389.5 to 427.5 meters below the seafloor, Cores 42–45: variably fractured and altered, high-MgO bronzite andesite of the boninite suite; and
- B₂: 427.5 to 465.5 meters below the seafloor, Cores 46–49: intensely fractured and altered tholeiitic basalt.

The rocks were originally divided into five lithologic units. It is now evident that the high degree of fracturing

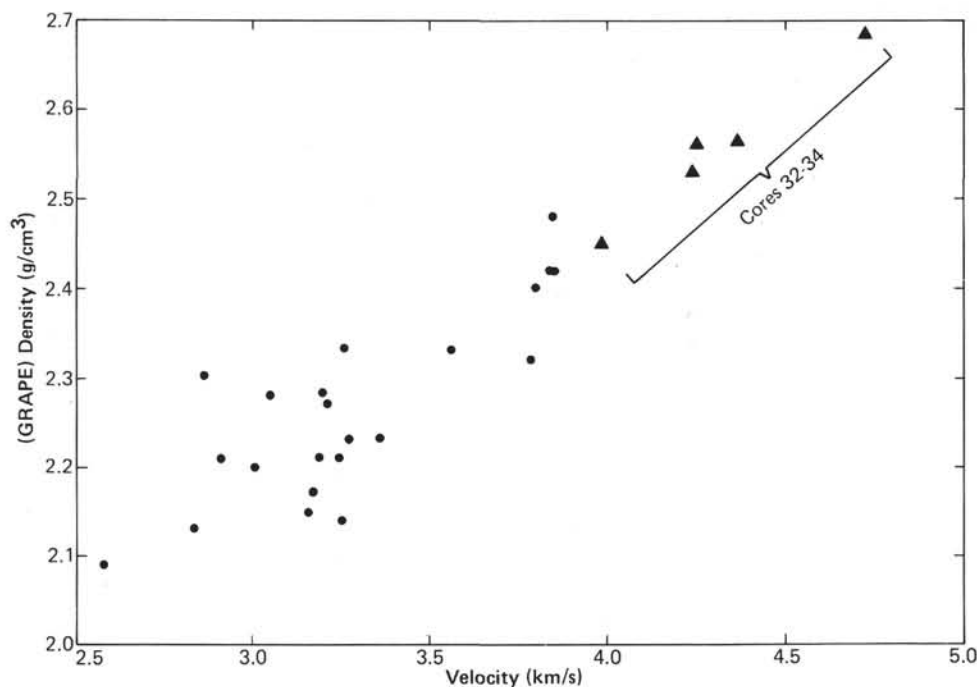


Figure 11. Sonic velocity (km/s) versus density (g/cm^3) for basalts, Site 458.

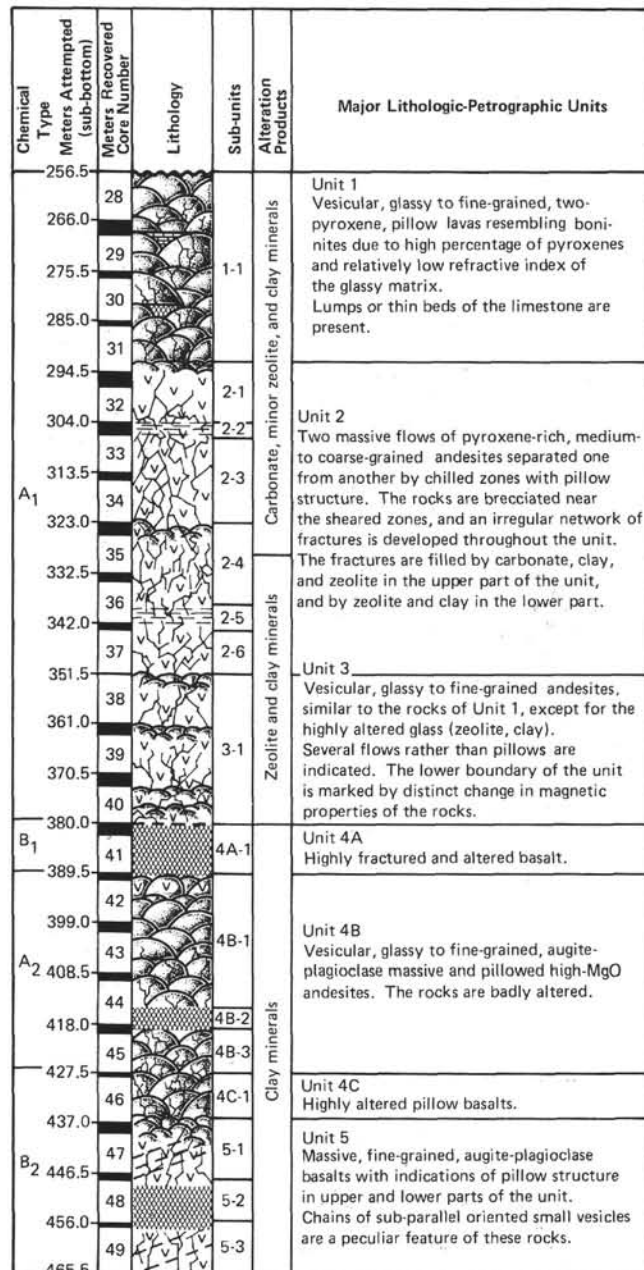


Figure 12. Igneous basement lithologic representation recovery, and unit descriptions, Site 458. Cross-hatched patterns represent zones of intense fracturing.

and alteration in the lower part of the hole made identification of petrographic types difficult. For this reason, Lithologic Unit 4 consists of two intervals of tholeiitic basalt separated by three cores containing boninite andesite. Clearly, some revision of lithologic units is necessary. However, several chapters in this volume make reference to the original shipboard lithologic units. In order to maintain internal consistency, the basic lithologic unit numbers are maintained, and alphabetic modifiers are assigned, based on the chemical contrasts within Unit 4. The new unit designations are as follow: Core 41 is Unit 4A (tholeiitic basalt); Cores 42-45 comprise Unit 4B (high-MgO andesite);

most of Core 46 is Unit 4C (tholeiitic basalt); and the rest of Core 46 through Core 49 is Unit 5 (tholeiitic basalt). Minor lithologic sub-units within the units are indicated numerically, as, for example, Unit 4B-1, on Figure 12. Descriptions of these units and sub-units (summarized in Table 4) are as follows:

Units 1 through 3 (total thickness 123.5 m) consist of several interbedded pillow sequences and more massive basaltic flows (Fig. 12). The rocks have abundant ortho- and clinopyroxenes. Petrographically, they resemble the high-magnesium andesites or boninites exposed in fairly similar geological situations on the Bonin Islands (Kuroda and Shiraki, 1975). Similar rocks, along with an ophiolite-like assemblage, were dredged in 1976 by the R/V *Dm. Mendeleev* from the island-arc wall of the Mariana Trench south of Guam (Dietrich et al., 1978). These, together with ophiolite-like rock assemblages, are also exposed on Cape Fogel, Papua-New Guinea (Dallwitz et al., 1966).

Unit 1 includes samples recovered in Cores 28 through 31 and represents the upper 37 meters of the igneous basement section (Fig. 12). The rocks are dark gray to dark greenish gray, dismembered fragments of pillows. The pieces that are more glassy and apparently represent outer pillow zones are usually more vesicular (20-40%; 0.1-5.0-mm diameter) than the fine-grained fragments of the pillow interiors (5-20%; 0.1-2.0-mm diameter). Many specimens of these rocks manifest irregular fractures cemented by carbonate, zeolite, and minor clay minerals. The main features of the rocks are fairly consistent throughout the unit. Several pieces of limestone recovered among the volcanic rocks apparently reflect the presence of lumps or thin beds of sediments within the pillow pile.

Unit 2 (Fig. 12) represents the next 58 meters of igneous basement and consists of two massive flows separated from one another by chilled zones indicative of pillow structures. Six sub-units are defined within Unit 2. These subdivisions are based on structural characteristics of the rocks as defined in Table 4. The massive rocks are medium- to coarse-grained, dark greenish gray, pyroxene-rich basalts. The grain size (0.1-1.0 mm) is fairly constant throughout the unit, but the chilled zones are more vesicular (10-20%; 0.1-3.0 mm diameter) than the inner zones of the flows (5-15%; 0.1-2.0 mm diameter). Two distinct, sheared zones are observed within the flows (see Table 4 and Fig. 12 for exact positions). The upper zone is marked by the presence of rock pieces with abundant slickensides. The lower one is represented by highly fractured and tectonized mylonites. The basalts are brecciated near the sheared zones and fairly fractured throughout the unit (total volume of chaotically disposed fractures is about 1-3%). Carbonate, zeolite, and minor greenish black clay minerals fill the fractures in the upper part of the unit, but below the middle part of Core 35 the carbonate disappears and only zeolites and clay occur as vein-forming material.

Unit 3 (Fig. 12), representing 28.5 meters of the section, consists of rocks similar in many aspects to the rocks of Unit 1. However, there are a greater number of flows present in the unit. The rocks show a higher

degree of alteration than those of Unit 2. The glassy matrix in these rocks is almost totally replaced by clay minerals and zeolites; carbonate is absent and minor native copper mineralization is observed in the rocks of Core 39. Large vesicles (up to 20 mm), which are irregular in shape and partly filled by clay, are sometimes observed in these rocks.

The lower part of the igneous section (total thickness penetrated is 85.5 m) consists of augite-plagioclase basalts and is now divided into three units. Unfortunately, the contact between the pyroxene-rich basalts of Unit 3 and these basalts was not recovered, and its nature remains uncertain. Units 1 through 3 are of normal magnetic polarity, whereas Units 4 and 5 are reversed.

Unit 4A represents 9.5 meters of cored igneous basement section. It consists of greenish black, fine- to medium-grained, highly altered and fractured basalt, all in Core 41.

Unit 4B consists of fragmental and fractured pillows (Sub-units 4B-1 and 4B-3) interbedded with intensely fractured rocks (Sub-unit 4B-2), which were probably originally fairly massive (Table 4). Because the pillows were recovered as separate pieces, whereas the fractured massive rocks represent a fairly compact mass, there was a likely different recovery rate for each rock type during drilling. Thus, it is difficult to estimate the thickness of these three sub-units. Small vesicles (0.1–2.5 mm in diameter) occupy up to 15 to 20 percent of the pillow fragments and are less abundant (2–7%) in the massive rocks of Core 44 (Sub-unit 4B-2). Unit 4C consists of fractured and altered pillows, resembling those of Unit 4B.

Unit 5 (representing the lowest 38 m of the hole) consists of very fine grained augite-plagioclase basalts with abundant subparallel trains of small vesicles (3–5%; 0.1–1.5 mm in diameter). The unit has been divided into three sub-units, since its middle part (Core 48) was recovered as a highly fractured, originally massive mass, while the rock pieces in upper and lower sub-units have distinct indications of pillow structure.

All the rocks of Units 4A, 4B, 4C, and 5, except some glassy pillow fragments, are extremely altered. They are brittle and soft and can be easily scratched even by a fingernail. Clay minerals form the main alteration product replacing the glassy matrix and mafic minerals.

Petrography

The petrography of volcanic rocks recovered from basement at Site 458 (256.5–465.5 m below the seafloor) is summarized in order of the units shown on Figure 12. A detailed consideration of crystal morphologies of rocks from Units 1 through 3 is given in Natland (this volume).

Unit 1 (Cores 28 through 31-1, Piece 17)

Rocks here are very fine grained to glassy, vesicular, two-pyroxene, high-MgO, bronzite andesites taken from pillow fragments. They have a high percentage of combined clinopyroxene microlites and micropheno-

Table 4. Basement lithologic units and sub-units, Site 458.

Unit 1:

Sub-unit 1-1—Cores 28–31-1 Piece 17(?)

Vesicular, fine-grained to glassy microphyric pillow lavas.

Unit 2:

Sub-unit 2-1—Cores 31-1 Piece 17–32-4

Massive, vesicular, aphyric, coarse-grained andesite.

Sub-unit 2-2—Core 33-1 Pieces 4–7

Zone of slickensided sheared rocks.

Sub-unit 2-3—Cores 33-1 Piece 8—end of Core 34

Massive, aphyric coarse-grained andesites, more fractured at base.

Sub-unit 2-4—Cores 35-1–36-2 Piece 7

Probably single cooling unit, near glassy at the top, medium- or coarse-grained toward base, with several zones of cemented breccia (originally fractured).

Sub-unit 2-5—Core 36-2 Piece 8—end of the core

Entirely fractured and sheared andesitic mylonite.

Sub-unit 2-6—Core 37

Fractured aphyric, medium-grained andesite (probable continuation of single cooling unit through Sub-units 4–6).

Unit 3:

Sub-unit 3-1—Cores 38–40

Sequence of fairly thin flows or large pillows. At least four cooling units indicated. Larger pieces invariably highly fractured, but cemented. Andesites are aphyric and near glassy, to medium-grained and heavily altered. Copper mineralization in Core 39.

Unit 4A:

Sub-unit 4A-1—Core 41

Dark gray-green, highly altered and fractured, probably originally fairly massive.

Unit 4B:

Sub-unit 4B-1—Cores 42–44-1 Piece 10

Dark gray-green, variolitic to fine-grained pillow fragments.

Sub-unit 4B-2—Core 44-1 Piece 95, 150 cm

Dark gray-green, highly altered and fractured basalts, probably originally fairly massive, similar to the rocks of Sub-unit 4-1.

Sub-unit 4B-3—Core 45

Same as Sub-unit 5-1.

Unit 4C and Unit 5:

Sub-units 4C-1 and 5-1—Cores 46 and 47, respectively.

Fairly thin massive flows or pillows. Probably two cooling units (boundary Section 47-1 Piece 12). Aphyric dark gray-green, altered, fine-grained basalts with sub-parallel trains of vesicles.

Sub-unit 5-2—Core 48

Highly fractured, once fairly massive, intensely altered basalts of type similar to the rocks of Sub-unit 5-1.

Sub-unit 5-3—Core 49

Similar to the Sub-unit 5-1.

crysts (15–45%) and no plagioclase microlites, although plagioclase spherulites are abundant in some samples. The refraction index of the glass, as determined in one sample, indicates it has SiO₂ > 60 percent. The rocks lacking plagioclase are petrographically similar to boninites (Kuroda et al., 1978; Meijer et al., this volume; Sharaskin, this volume), and contain up to 5 percent Mg-rich orthopyroxene (bronzite compositions), and diopside augite microphenocrysts, which sometimes are intergrown with orthopyroxene or pigeonite. The Mg-rich orthopyroxene compositions are an important point of similarity to boninites.

Unit 2 (Core 31-1, Piece 18 through Core 37)

Generally, medium- to coarse-grained, one and two-pyroxene intersertal to subophitic basaltic lavas from two massive flows; the top of the second flow (Section 35-2) is fine-grained and spherulitic. Plagioclase in the basalts is abundant, fairly calcic (ranging from An_{60} to An_{72}), and its proportion to clinopyroxene (1:1 to 3:1) is typical of basalts or even basaltic andesites. Unit 2 basalts contain minor orthopyroxene—again the magnesian varieties seen in Unit 1. The interior of the upper flow (Core 33) is virtually holocrystalline, but has less than 25 percent clinopyroxene, and an abundant patchy interstitial feldspar at least as sodic as oligoclase, but present only in small quantities in the same flow above and below. This feldspar is associated with minor quartz in Core 33 (but it is not certain how much of this is primary). Quartz also occurs at the bottom of Core 31. The interior of the flow appears to be more fractionated than the top or bottom, based mainly on the abundance of feldspar (especially the interstitial type) relative to clinopyroxene.

Unit 3 (Cores 38–40)

This is a sequence of at least four cooling units, probably thin flows, with near-glassy rims and fine-grained interiors. Available thin sections, mainly from glassy or near-glassy rims, include clinopyroxene-rich, plagioclase-poor basalts similar to Unit 1. Others contain more plagioclase and are coarser grained. Alteration is intense, generally having transformed glass to clays and/or zeolites. But the clinopyroxenes, which are mainly microlitic, have not been affected in the glassy rocks.

Units 4A, 4C, and 5 (Cores 41 and 46–49)

Both these units contrast sharply with Units 1 through 3 having abundant (10–50%) acicular plagioclase microlites, and subordinate augite pseudomorphs now altered to clays (Tr —6%; plagioclase:augite = 2:1 to 10:1). They also are generally less vesicular. The plagioclases are set in an altered, once-glassy, mesostasis. Some have subparallel plagioclase microlites (pilotaxitic texture), aligned by flow. The mesostasis in some samples is rich in titanomagnetite, compared with basalts of Units 1 through 3.

Unit 4 consists mainly of pillow fragments, whereas Unit 5, although very fine grained, lacks glassy rinds and variolitic zones. The grain size of most of the samples in these two units is highly uniform, suggesting massive flows. Petrographically, the two units are very similar, but Unit 5 basalts have distinct sub-parallel vesicle chains along which secondary reddish iron oxides are concentrated. These no doubt correspond to the fine, platy partings visible in hand-specimens.

All three of Units 4A, 4C, and 5 contain rocks with minor plagioclase (An_{72}) and clinopyroxene microphe-nocrysts, but the dominant feldspar is microlitic plagioclase of sodic labradorite composition (An_{55}). The plagioclase is not sufficiently sodic for the rocks to be called andesite, but is more sodic than in typical basalts. The

rocks could thus be called either basalts or basaltic andesites.

Unit 4B (Cores 42–45)

Only two thin sections of rocks from this lithologic unit were prepared. One is badly altered and spherulitic with clinopyroxene microlites and swirls of tiny plagioclase needles. The other is intersertal with about 50 percent plagioclase crystals, lesser clinopyroxene, some opaques and an altered mesostasis. Neither thin section has the distinctive orthopyroxenes of Units 1 through 3 that would have allowed ready identification of them as bronzite andesites. This undoubtedly was the source for the shipboard misidentification of rock types leading to the original scheme of lithologic units.

Alteration

Nearly all of the igneous rocks recovered at Site 458 show considerable alteration effects. The pattern of alteration displayed in these rocks is fairly systematic with depth (Fig. 13), although a significant discontinuity in the degree of alteration occurs at the level of Core 36, and other minor discontinuities may be present. In general, dioctahedral smectite and phillipsite are the dominant secondary minerals (Natland and Mahoney, this volume), with carbonate and silica minerals present locally.

Clay minerals occur throughout the cored interval. Their color ranges from apple-green to brown to clear, although this variation does not correlate systematically with depth. In Cores 28 and 29, clay occurs primarily as a thin vesicle lining and as a minor alteration product of glass and clinopyroxene, particularly along fracture surfaces. Its abundance increases in Cores 30 and 31 and then gradually decreases down to Core 35. In Core 36, the clay content increases dramatically, especially within the shear zone. It stays relatively high to the bottom of the hole, although a few fresh glassy pillow rinds are preserved free of clay in Cores 46 and 48. In cores from Core 36 downward, the clay is an alteration product of the mesostasis and clinopyroxene. Clays in the lowest cores (e.g., Section 46-1) may have a significant chlorite component as indicated by their more definitive crystal form, texture, and anomalous birefringence. Mixed-layer smectites were identified by X-ray diffraction in Cores 44 and 49. It is worth noting that the increased clay content of the rocks below Core 35 caused extensive fracturing during drilling and eventually led to abandonment of the hole.

The zeolite content of these rocks also shows some interesting trends (see Fig. 13). From Core 28, Section 1, where zeolite first appears as a vesicle lining, the zeolite content gradually increases down to Core 35. In this interval, zeolite increasingly replaces glass and lines vesicles and veins with a concomitant decrease in the abundance of clay. Interestingly, the feldspars appear to remain relatively unaffected by alteration even in the zones of high zeolite abundance. In Cores 31 through 33, a uniaxial mineral with low birefringence, which appears to be quartz, joins the zeolite in the mesostasis.

Meters Attempted (sub-bottom)	Meters Recovered Core Number	Lithology	Sub-units	Alteration Minerals								
				Volume Percentage of Rock								
				Clay		Zeolite		Carbonate		Vesicles		
10	30	10	30	2	6	10	30					
256.5	28			X		X			X		X	
266.0	29			XX		XX		X	XX		X	
275.5	30		1-1	XXX		X			XX		XX	
285.0	31			X		X			XX			
294.5	32		2-1	X		X		X	XXX			
304.0	33		2-2	XX		X		X	XX			
313.5	34		2-3	X		X		X			X	
323.0	35			X		X		X	XX			
332.5	36		2-4	X		X						
342.0	37		2-5	X		X			XX			
351.5	38		2-6	X		X			XX			
361.0	39		3-1								XX	
370.5	40			X		X			XX			
380.0	41		4A-1	X		X			XX			
389.5	42											
399.0	43		4B-1	X		XX			XX			
408.5	44		4B-2									
413.0	45		4B-3									
427.5	46		4C-1			X		X	X			
437.0	47		5-1									
446.5	48		5-2						X			
456.0	49		5-3									
465.5												

Figure 13. Occurrence of alteration minerals observed in thin sections of igneous rocks, Site 458.

However, this mineral is rare, if not absent, in cores below this interval, and may have formed deuterically. The composition of the zeolite(s) observed in cores from this site was not readily determined on the basis of thin-section study, but phillipsite was repeatedly identified

by X-ray diffraction (Natland and Mahoney, this volume).

A carbonate phase, probably calcite, is present in Cores 28 through 35 as a vein filling, occasionally as a vesicle lining, and rarely as a replacement product of the mesostasis. This phase appears to be absent below Core 35 on the basis of tests with acid and thin-section study. In Core 30, Section 2, a fragment of limestone was found included within the basaltic rock. Its contact relationships with the basalt are sharp, and very little, if any, recrystallization or metasomatism along this contact is evident in thin section.

It is worth noting that, notwithstanding that most veins are completely filled with secondary minerals, and the mesostasis of the basalts is often completely replaced, vesicles in these basalts (although generally abundant) are rarely filled with secondary minerals. In most cases, secondary minerals are restricted to a thin lining of the vesicle wall or a limited protrusion of crystals, particularly of zeolite, into the vesicle cavity.

One additional mineral identified by X-ray diffraction is palygorskite, occurring in Core 28 at the top of basalt. Also, native copper associated with smectites occurs in Core 39.

In conclusion, the igneous rocks of Site 458 have undergone varying degrees of low-grade alteration. The association of dioctahedral smectite with phillipsite suggests a dominantly oxidative alteration. Some transformation to mixed-layer clays has occurred, implying continued diagenesis. The palygorskite, however, probably formed earlier, before significant burial, under oxidative and possibly hydrothermal conditions (Natland and Mahoney, this volume). The products of these secondary effects generally increase in abundance downward in the hole. A reversal from a zeolite- to a clay-dominated assemblage occurs below Core 38. Slickensides in clay-rich shear zones suggest tectonic displacement of the igneous stratigraphy at several depths in the hole. One such displacement is evidenced by a substantial shear zone (~0.6 m) of nearly pure slickensided clay and an increase in fracturing of the rocks directly above this zone. Tectonic displacement is also suggested by the presence of fresh glass at the deepest levels in the hole (e.g., Core 48, Section 1).

Chemistry

Combining the data of Wood et al., Bougault et al., Sharaskin, and Hickey and Frey (all in this volume), there are four primary chemical types among these rocks, as outlined under "Igneous Rock Lithology." Lithologic Units 1 through 3 are essentially one chemical type (A₁), although there is some compositional variation within the lavas suggesting that more than one eruptive event may have produced these rocks. The lavas have fairly high SiO₂ (51.5–59.8%), yet surprisingly low and uniform TiO₂ (0.28–0.37%) and Zr (28–39 ppm). Despite the high SiO₂, many of the rocks analyzed have surprisingly high MgO (up to 9.36%) and Cr (168–290 ppm). These are the identifying chemical characteristics of lavas of the boninite type (e.g., Wood et al., this

volume). However, the Site 458 lavas with these characteristics are not as magnesian nor rich in Ni and Cr as boninites from the type locality in the Bonin Islands (Kuroda and Shiraki, 1975), nor do they have clinostatite, a mineral found in many boninites (e.g., Dallwitz, 1968). Kushiro (this volume) argues from melting experiments on two Site 458 samples that, unlike true boninites, they cannot have been derived from direct melting of peridotite in the mantle. Instead, a fair amount of fractionation of olivine and orthopyroxene from an original parent appears to have occurred to give the Site 458 compositions. For these reasons, we here term these rocks high-MgO, bronzite andesites, or more simply, bronzite andesites, and identify them as members of the boninite series (e.g., Meijer et al., this volume).

Within Units 1 through 3, comprising type A₁, there are some chemical variations. However, Zr and TiO₂, which are useful in defining chemical stratigraphy among seafloor basalts, are here both so low and uniform that they are useless for this purpose. Other immobile trace elements, such as Y and Nb, are similarly low and uniform, and cannot be used for identifying chemical sub-units. Major oxides which are sensitive to such magmatic processes as crystal fractionation—including CaO, K₂O, and MgO—are also sensitive to alteration processes, which have been extensive in these rocks. Consequently, although chemical differences undoubtedly caused by magmatic processes can be distinguished among fresher bronzite andesite samples, it is difficult to define precise chemical boundaries; there is little sample-to-sample consistency.

We do note the following contrasts among fresher samples. Low-SiO₂ (52.0–53.1%), high-MgO (8.97–9.71%) lavas occur at two intervals—namely, Core 29, and Cores 39 and 40. These are samples with more typically boninite-type petrography; that is, they have abundant clinopyroxene microlites, phenocrysts of magnesian orthopyroxene, but no plagioclase. They have little or no normative quartz. The massive lavas of Cores 31 through 35 have considerably higher SiO₂ (56.9–59.8%) than these, and lower MgO (4.62–5.53%). They are coarse-grained samples carrying interstitial quartz and have 7.3 to 14.2 percent normative quartz. In the midst of these, however, there is one sample (in Core 33, Section 2) with both high SiO₂ (59.1%) and high MgO (8.13%), perhaps a sample with cumulus pyroxenes, which nevertheless still has high normative quartz (11.3%).

Lithologic Unit 4B is a second interval of bronzite andesite (chemical type A₂) separated from the type A₁ bronzite andesites by a single core of basalt (Core 41, lithologic Unit 4A, chemical type B₁). Type A₂ andesites share the general chemical characteristics of type A₁, except that TiO₂ is higher (0.49–0.56%), and Ni (65–82 ppm) and Cr (157–176 ppm) are lower, although there is some overlap for Ni and Cr. These samples appear more uniform in composition than type A₁ samples, and compare most closely to the low-MgO samples of that type.

The basalts of lithologic units 4A (chemical type B₁) and 4C plus 5 (chemical type B₂) can be clearly distinguished from the bronzite andesites by their higher TiO₂

(1.04–1.16%), Y (20–31 ppm), and Zr (47–111 ppm), and their lower Ni (11–28 ppm) and Cr (10–16 ppm), although there is some overlap. MgO in these samples is generally lower (3.73–7.96%) than in bronzite andesites with comparable SiO₂. Type B₂ basalts have over 13 percent total iron as Fe₂O₃, and could be termed ferrobasalts (Wood et al., this volume). The lower iron in the single analysis of type B₁ seems contradicted by the low MgO of that sample. This may in part be the result of alteration, but that sample also has the highest Zr (111 ppm), Na₂O (5.7%), K₂O (1.52%), and Ce (15 ppm) of all the samples analyzed from this hole. On these grounds, it could be considered the most fractionated basalt of the lot. In any case, it is a distinct chemical type, clearly different from Type B₂ basalts. Therefore, since there are both two distinct bronzite andesite compositions and two distinct basalt compositions, none of the major chemical types appears to represent a replication of any other unit by faulting. In all likelihood, the basement stratigraphy at Site 458 is one of eruptive sequence, despite the lithologic indications for extensive faulting of the rocks.

The effect of alteration on the lava compositions is difficult to separate from the effects of primary petrogenetic variations. Examining oxides or elements indicative of formation of K-bearing clay minerals, it is possible that alteration produced complementary threefold enrichments in K₂O and Rb, and twofold enrichment in Ba, among samples analyzed of basalt type B₂. In these same rocks, in which TiO₂ is nearly constant, there are differences of almost 2 percent in MgO and 1.6 percent in CaO that could have been produced by alteration. The bronzite andesites, which probably had very low Rb abundances to begin with, show a factor of 10 variation in this element, and a nearly threefold variation in Ba and K₂O. The same samples, however, show little variation in CaO or MgO despite the strong sample-to-sample fluctuations in K₂O, Rb, and Ba. This may reflect downhole variations in secondary clay mineral compositions and abundance.

PALEOMAGNETISM

Site 458 is located in the Mariana fore-arc area on a negative magnetic anomaly surrounded by a series of positive anomalies. Because of severe drilling disturbance, paleomagnetic measurements were possible only for the lowest sediment section (Cores 25–27) and the underlying igneous sections. The samples from the deepest two cores (Cores 46 and 47) showed a drastic increase in NRM intensity (reverse polarity); this may possibly explain the negative anomaly if such intensities continue to sufficient depths. Inclinations are negative and shallow (~ -15°) in the igneous section below 380 meters sub-bottom, and are positive and steeper (~ +30°) in the upper igneous section. Some tectonic event involving tilting of the upper section may explain this change in the inclination (Bleil, this volume).

SUMMARY AND CONCLUSIONS

Site 458 was drilled with the objectives of determining the sedimentary history as well as the petrology and

physical state of the igneous basement of the Mariana fore-arc region.

The geophysical setting of Site 458 is also of particular interest. The hole was located on the southeastern periphery (about 8 km west of center) of a sharp positive gravity anomaly. Profiler records indicated somewhat over 200 meters of sediment at the site. Magnetic anomalies in the area are complex, but a reversely oriented dipole type anomaly (ca. 200 γ in total amplitude) appears to be associated with the target gravity anomaly.

A total penetration of 465.5 meters with a core recovery of 97.8 meters (recovery rate 21%) was attained at this site. The upper 256.4 meters comprised sediments, and the lower 209 meters igneous rocks.

Two temperature measurements, at 76.0 and 142.5 meters below the seafloor, provide a heat flow value of about 0.6 HFU, although there were difficulties in interpreting the temperature records. Sediment conductivity was found to increase with the sub-bottom depth at a rate of 0.23 mcal/cm s°C/100 meters, a rate comparable to those at other Leg 60 sites and also to that reported by Hyndman et al. (1974) for DSDP Leg 26 sites in the Indian Ocean. The thermal conductivities of both sedimentary and igneous rocks at this site show a distinct correlation with the lithologic units, especially with the degree of alteration.

The sediments encountered at this site are, from the top downward, mainly siliceous mud, nannofossil ooze, and chalk. The sediments range from Pleistocene to early Oligocene in age as determined from well-developed nannofossil and radiolarian assemblages. The basement sections recovered beneath the sediments are interbedded pillows and massive flows of two distinct rock types: (1) island-arc-related tholeiitic basalt, and (2) high-magnesium, bronzite andesites.

Although highly fractured and exhibiting numerous slickensided surfaces, the degree of tectonic displacement of these rocks is probably not great. Paleomagnetic directions in the rocks indicate that what tectonic tilting has occurred, has been subdued and involved large bodies of rock. Basement Lithologic Units 4A, 4B, 4C, and 5 (380–465.5 m sub-bottom) have an average inclination of -15° (reversed direction), whereas the upper igneous Units 1 through 3 (256.5–380 m sub-bottom) have an average inclination of about $+30^\circ$ (positive direction). Thus, it appears that there may be some rotation between the two sets of rock, but there does not seem to be much small-scale disruption. Furthermore, comparison of the igneous geochemistry of the rock units shows that there is no repetition of the chemical units in the section.

Although no intercalated sediment layers were recovered, traces of limestone and sediments on the surfaces of the rocks recovered from the basement at Hole 458 suggest that this pile of flows and pillow lavas was extruded over a long enough period for some sedimentation to occur between igneous events. The single unidentified magnetic reversal in the igneous rocks further indicates that the section was emplaced over a period that is perhaps on the order of a million years.

The unusual rock types recovered in Hole 458 are discussed in detail in this volume by Meijer et al., Wood et al., Sharaskin, Hickey and Frey, and Kushiro. The rocks are termed high-MgO, bronzite andesites, and are specified as belonging to the boninite suite. Although sharing many of the petrographic and geochemical characteristics of true boninites, they are not sufficiently magnesian and lack both olivine and clinoenstatite—two minerals which occur in boninites. The Site 458 bronzite andesites, in fact, appear to be derived from a boninite parent by fractional crystallization (Kushiro, this volume).

Lavas of the boninite suite are more ubiquitous in this fore-arc setting than first thought. Even the vitric sands and tuffs recovered just above basement (Core 27) in Hole 458 have exceptionally high MgO and Cr contents (Wood et al., this volume), and could have had a boninite provenance.

It is interesting to note that the degree of alteration of the igneous section increases with depth, and is especially concentrated along zones of intense fracturing. Alteration was both oxidative and non-oxidative, with the latter being more extensive. Alteration minerals are principally dioctahedral smectites and phillipsite, with some carbonate veins. The increased alteration with depth has produced decreases in both seismic velocity and density with depth in samples taken from igneous basement. The relatively low velocities (3–4 km/s) and densities (2.1–2.5 g/cm³) of the Hole 458 basement rocks do not satisfy the geophysical anomalies which originally lured us to Site 458. The rocks below those we cored must therefore become considerably less altered and fractured, or have much greater initial densities, within a short distance.

The sediments in Hole 458 depict a history of nearly constant, relatively undisturbed sedimentation. A ~4-m.y. hiatus occurred in late Miocene/early Pliocene times, but three other possible hiatuses (middle Miocene, early Miocene, late Oligocene) are only 1.5 m.y. or less in duration. Some reworking of the sediments occurred during the Oligocene and middle Miocene, with even some chert fragments and igneous pebbles recovered in Core 12. However, there are no extensive turbidite sequences and no repeated sections. When compared to Site 451 (West Mariana Ridge, Kroenke, Scott, et al., 1980), which would have been close by before the opening of the Mariana Trough, Site 448 (Palau-Kyushu Ridge), which would have been nearby before the opening of the Parece Vela Basin, and even Sites 292 (Benham Rise) and 445 (Daito Ridge), the types and style of sedimentation are similar. Thus the Mariana fore-arc is, not surprisingly, similar to the other "old" ridges of the Philippine Sea region.

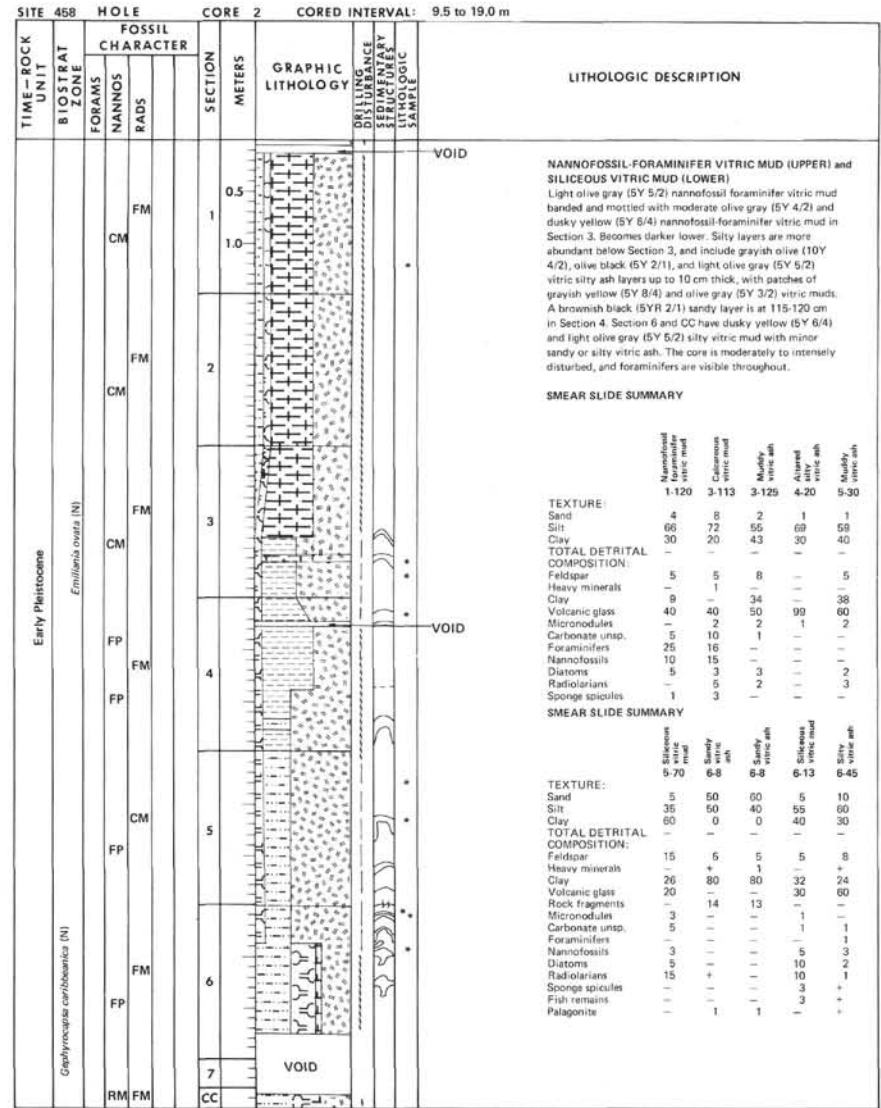
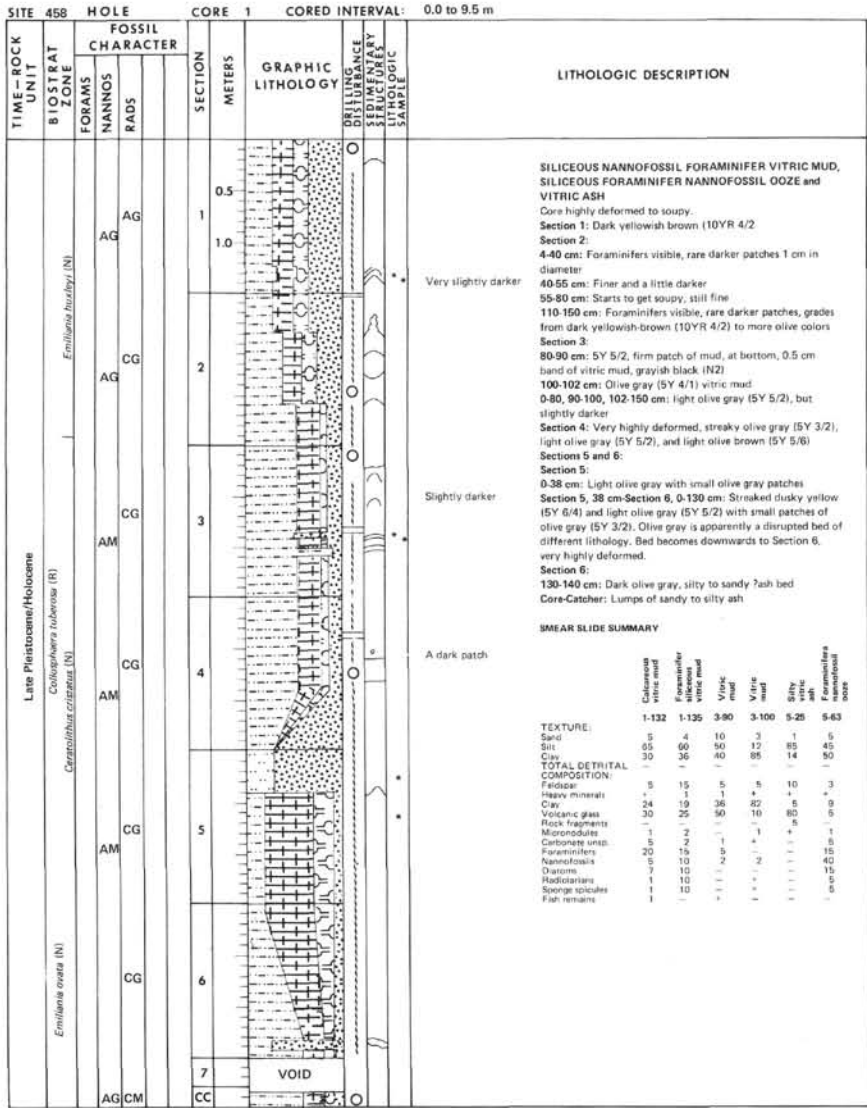
Volcanic ash and glass are ubiquitous in the sediments of Hole 458. The amount of volcanogenic material in the sediment declines after the basal lower Oligocene vitric tuffs, quickly reaching a minimum in the nannofossil chalks of the uppermost lower Oligocene, increasing slowly but remaining low in the upper Oligocene and through the lower Miocene, increasing somewhat in the middle Miocene, then jumping to the

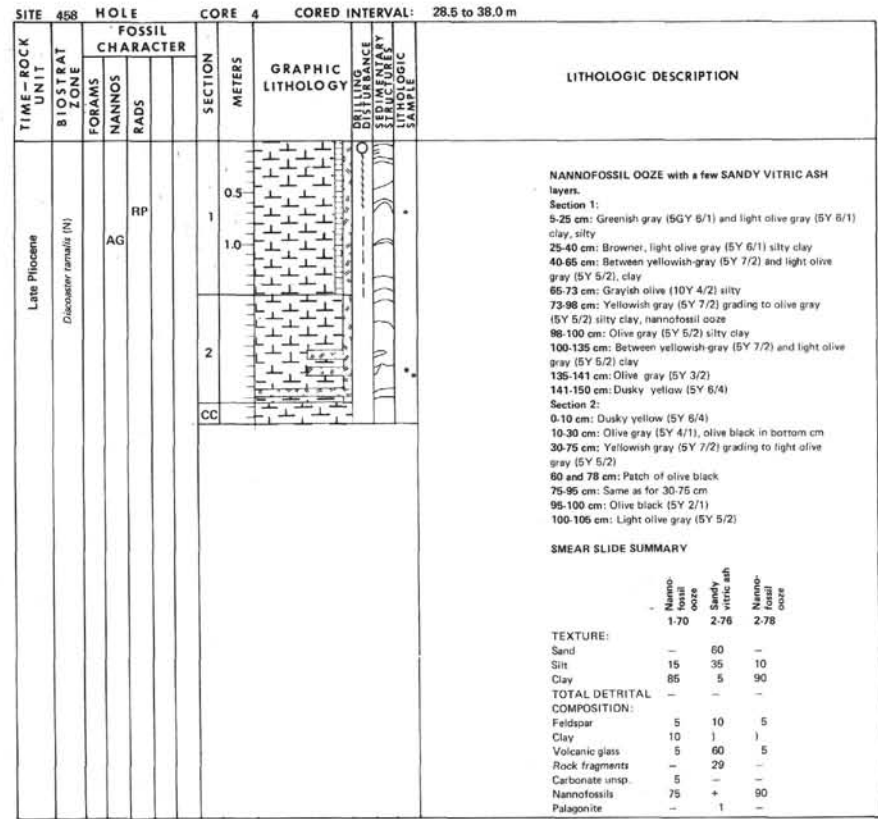
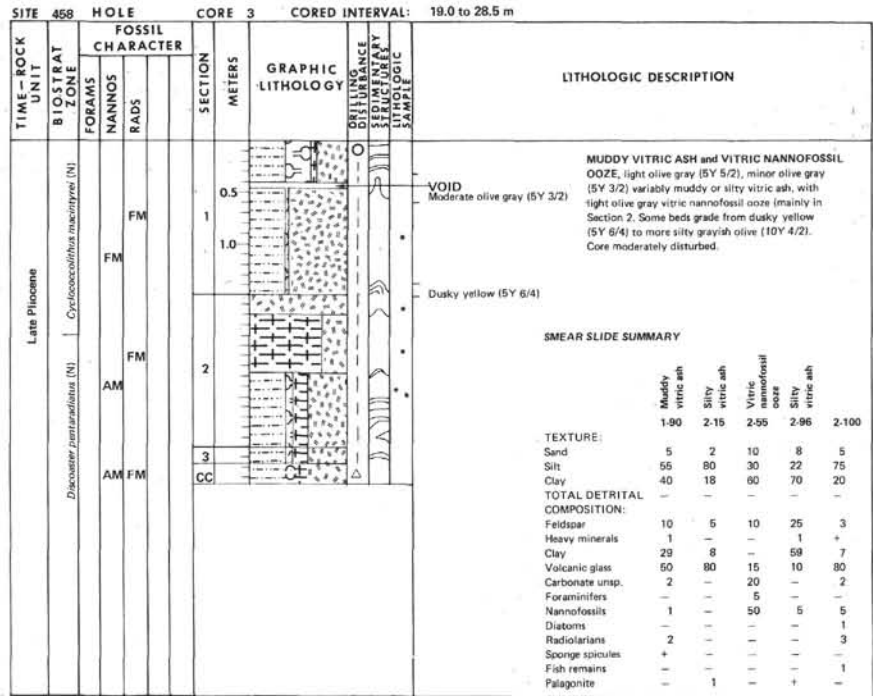
present high levels in the upper Miocene. The abundant volcanic ash in the upper Pliocene and Pleistocene was probably supplied from the present Mariana volcanic arc. In contrast to the trough sites west of the spreading axis of the Mariana Trough (Sites 453 and 454), Site 458 and the sites to the east of the axis (Sites 455 and 456), do not show any appreciable upward decrease of volcanic ash during this period. This seems to indicate that the volcanic activity of the Mariana arc has probably remained at more or less the same level. If this inference is correct, the Pleistocene decrease of volcanic components observed in the western Mariana Trough sites can be attributed to the increased distance of those sites from the volcanic arc, rather than a decline of the volcanic activity of the arc during the past 5 to 6 million years.

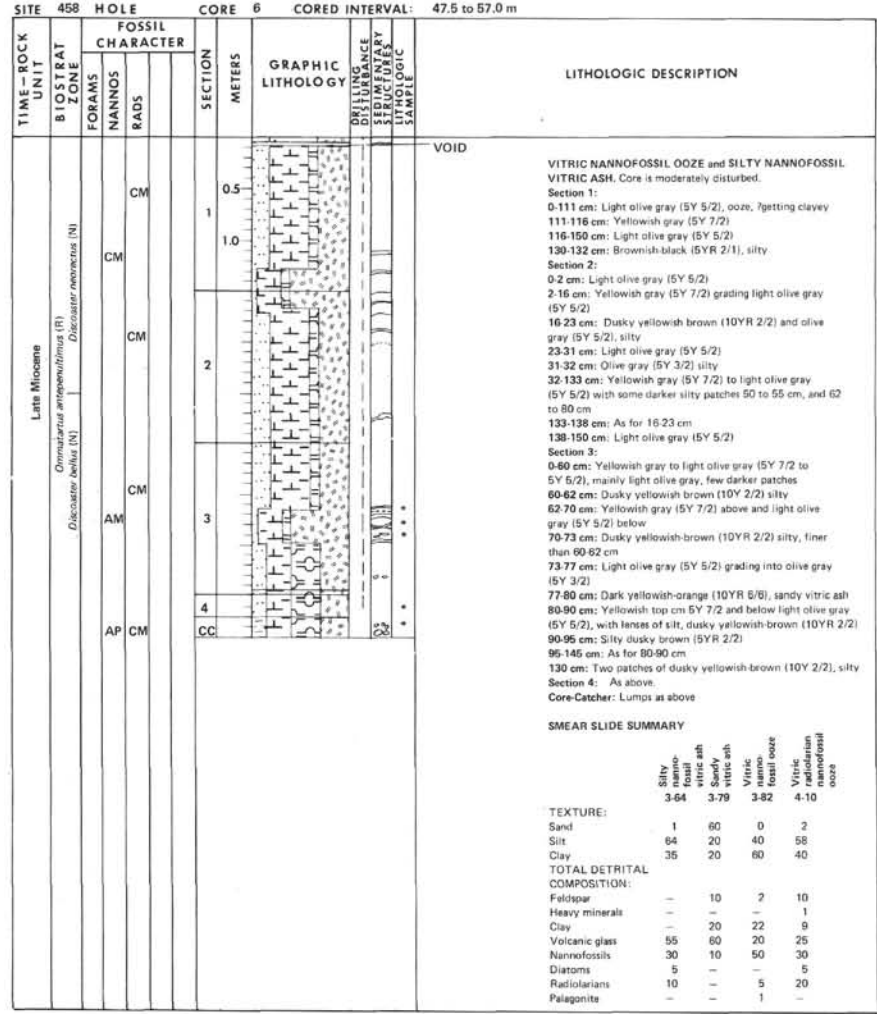
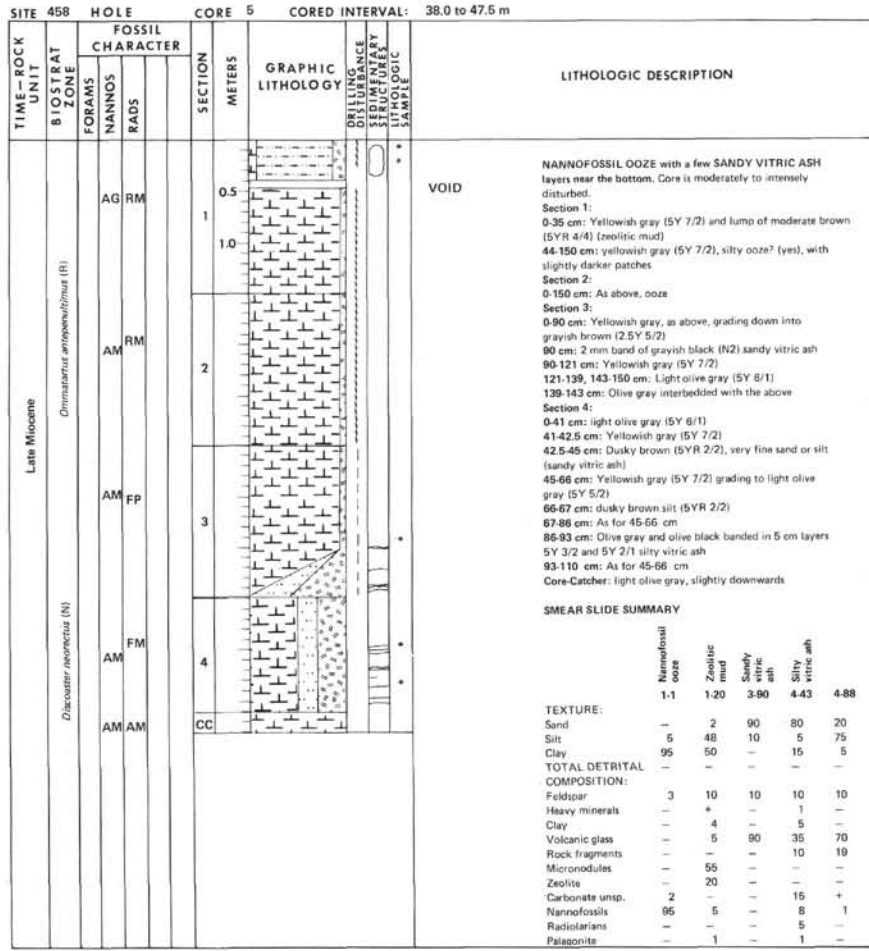
We see no correlation between the occurrence of back-arc spreading and the level of volcanic activity on the Philippine Sea arcs based on the sediments of Site 458.

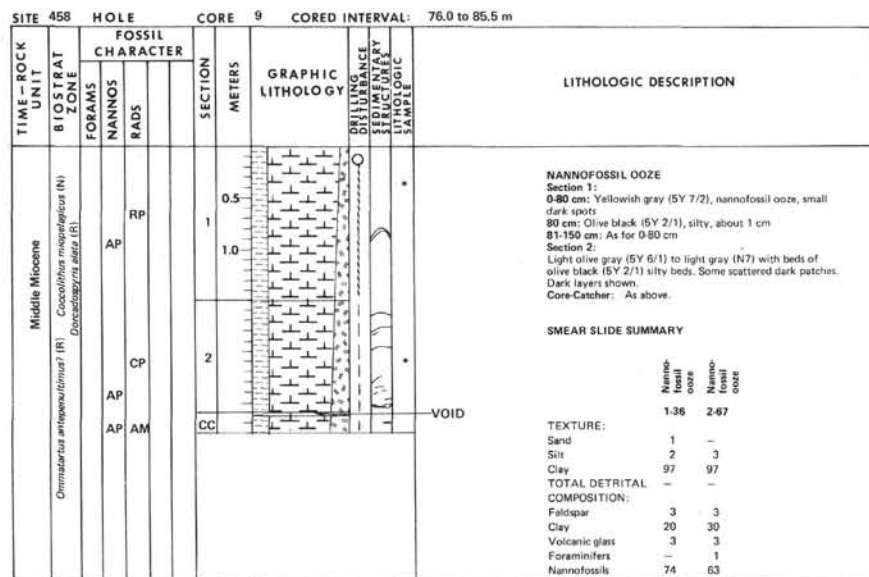
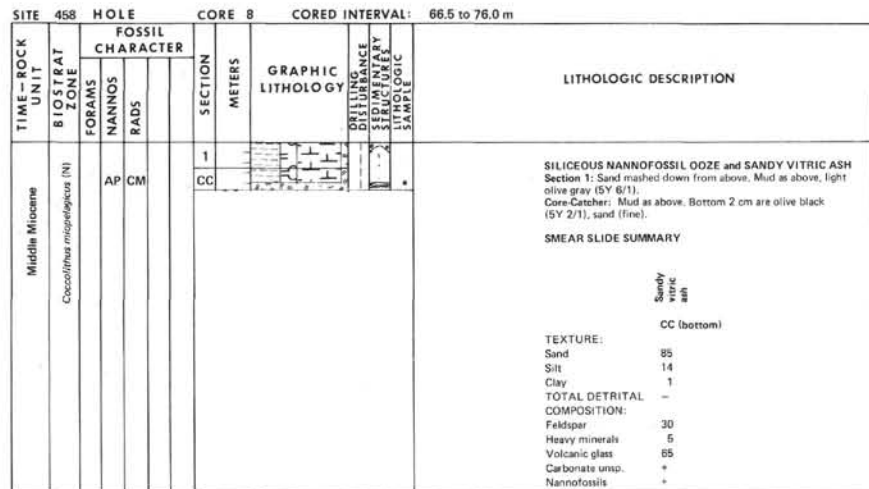
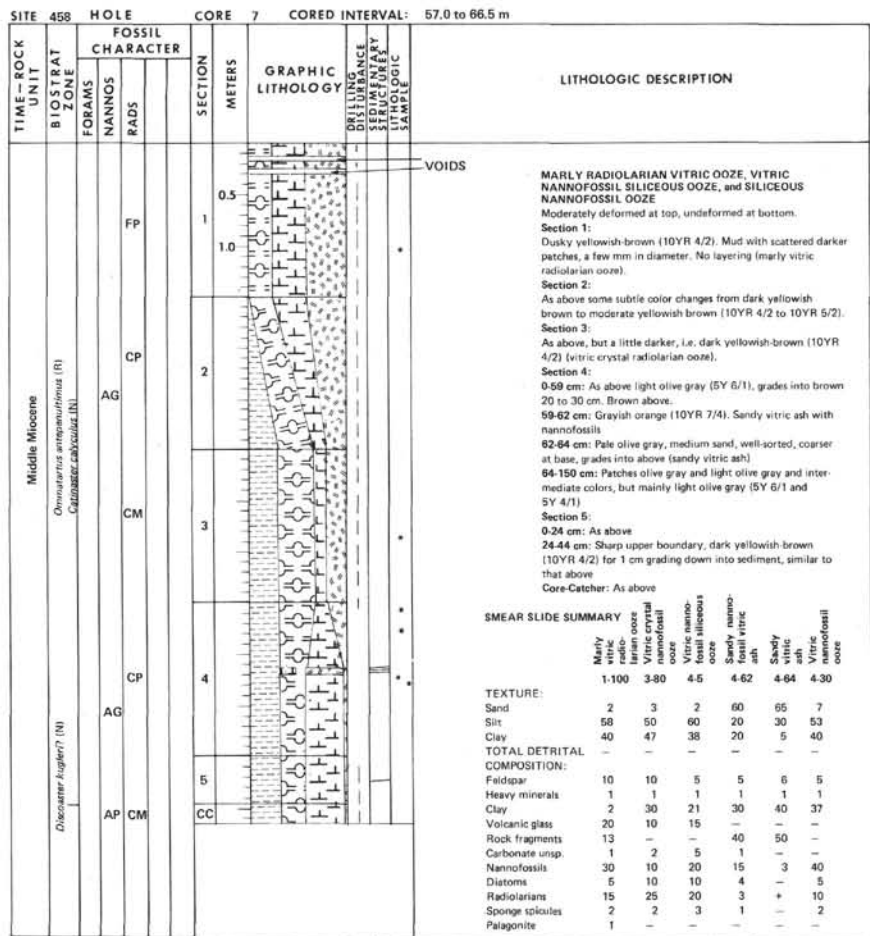
REFERENCES

- Dallwitz, W. B., 1968. Chemical composition and genesis of clinostatite-bearing volcanic rocks from Cape Vogel, Papua—a discussion. *Proc. 23rd Geol. Congr.*, 2:229–242.
- Dallwitz, W. B., Green, D. H., and Thompson, J. E., 1966. Clinostatite in a volcanic rock from the Cape Vogel area, Papua. *J. Petrol.*, 7:375–403.
- Dietrich, V., Emmermann, R., Oberhansli, R., et al., 1978. Geochemistry of basaltic and gabbroic rocks from the west Mariana basin and the Mariana trench. *Earth Planet. Sci. Lett.*, 39:127–144.
- Ellis, C. H., 1975. Calcareous nannofossil biostratigraphy—Leg 31, Deep Sea Drilling Project. In Karig, D. E., Ingle, J. C., et al., *Init. Repts. DSDP*, 31: Washington (U.S. Govt. Printing Office), 655–676.
- Hyndman, R. D., Erickson, A. J., and Von Herzen, R. P., 1974. Geothermal measurements on DSDP Leg 26. In Davies, T. A., Luyendyk, B. P., et al., *Init. Repts. DSDP*, 26: Washington (U.S. Govt. Printing Office), 451–464.
- Karig, D. E., 1971. Structural history of the Mariana Island arc system. *Geol. Soc. Am. Bull.*, 82:323–344.
- Kroenke, L., Scott, R., et al., 1980. *Init. Repts. DSDP*, 59: Washington (U.S. Govt. Printing Office).
- Kuroda, N., and Shiraki, K., 1975. Boninite and related rocks of Chichijima, Bonin Islands, Japan. *Rep. Fac. Sci. Shizuoka Univ.*, 10:145–155.
- LaTraille, S. L., and Hussong, D. M., 1980. Crustal structure across the Mariana Island Arc. In Hayes, D. E. (Ed.), *The Tectonic and Geologic Evolution of Southeast Asia: Geophys. Monog. Ser. 22*: Washington (American Geophysical Union), 209–222.
- Minster, J. B., and Jordan, T. H., 1978. Present-day plate motions. *J. Geophys. Res.*, 83:5331–5345.







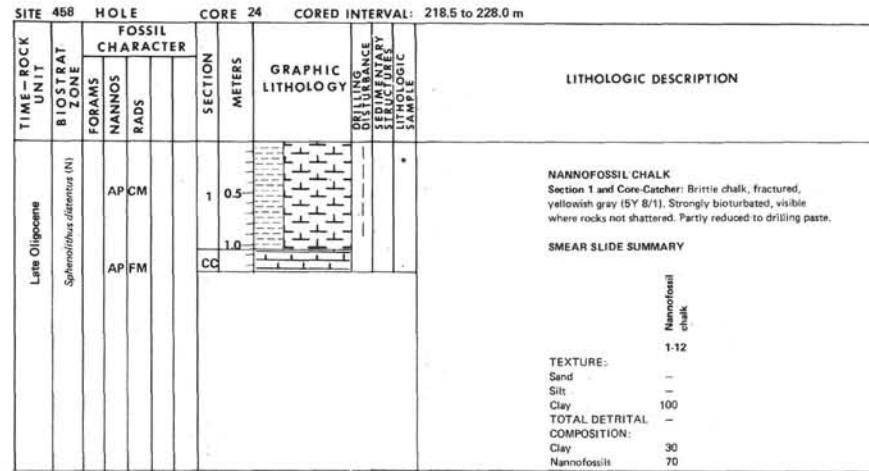
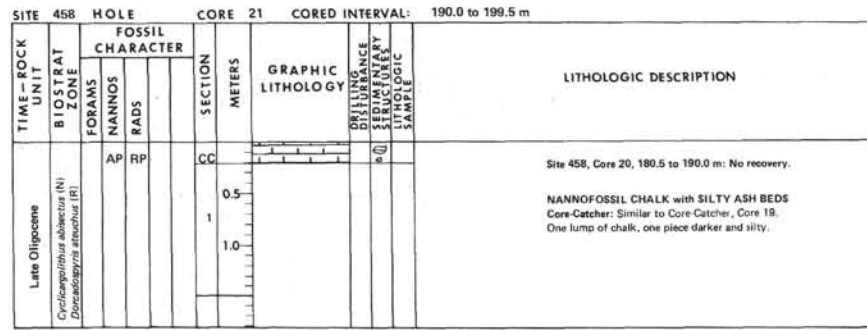
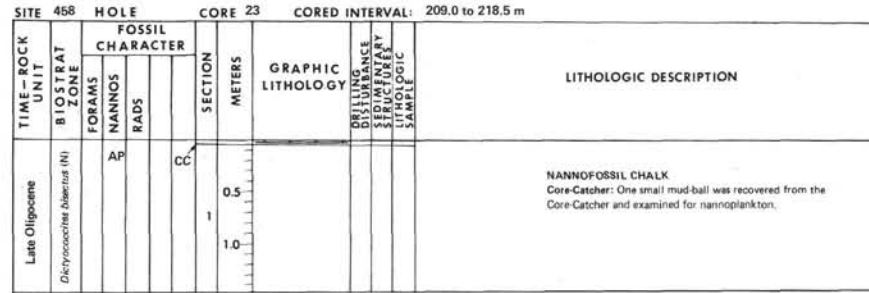
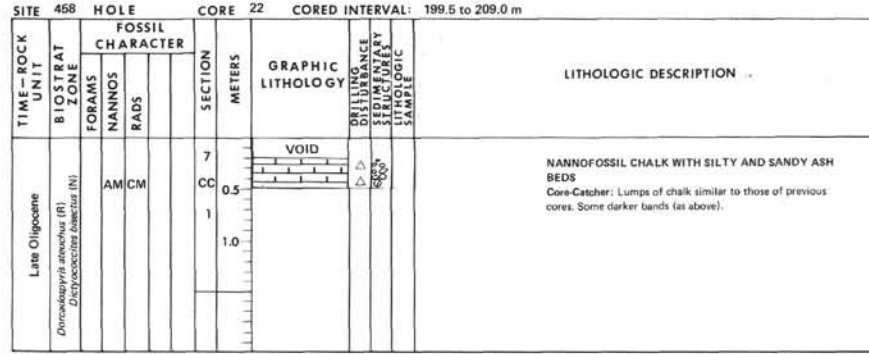
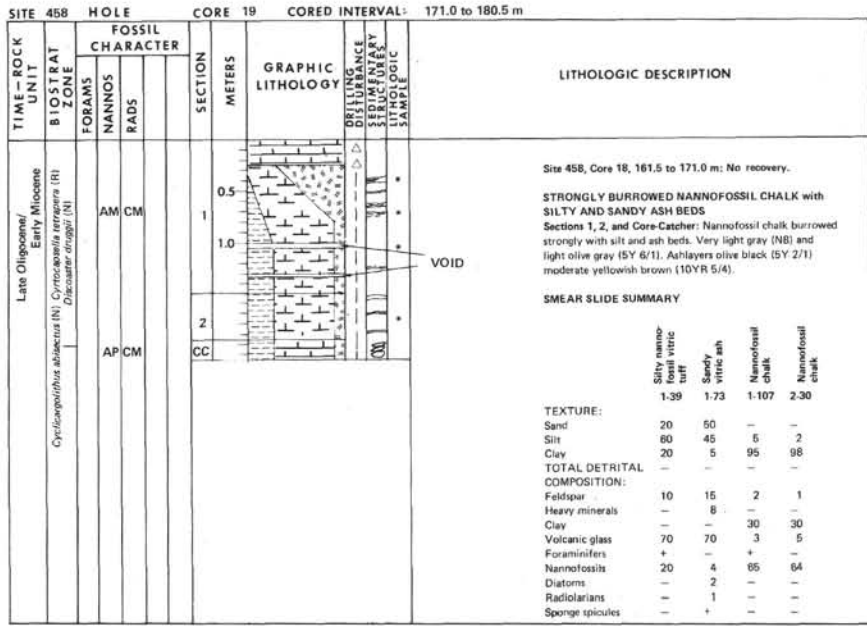


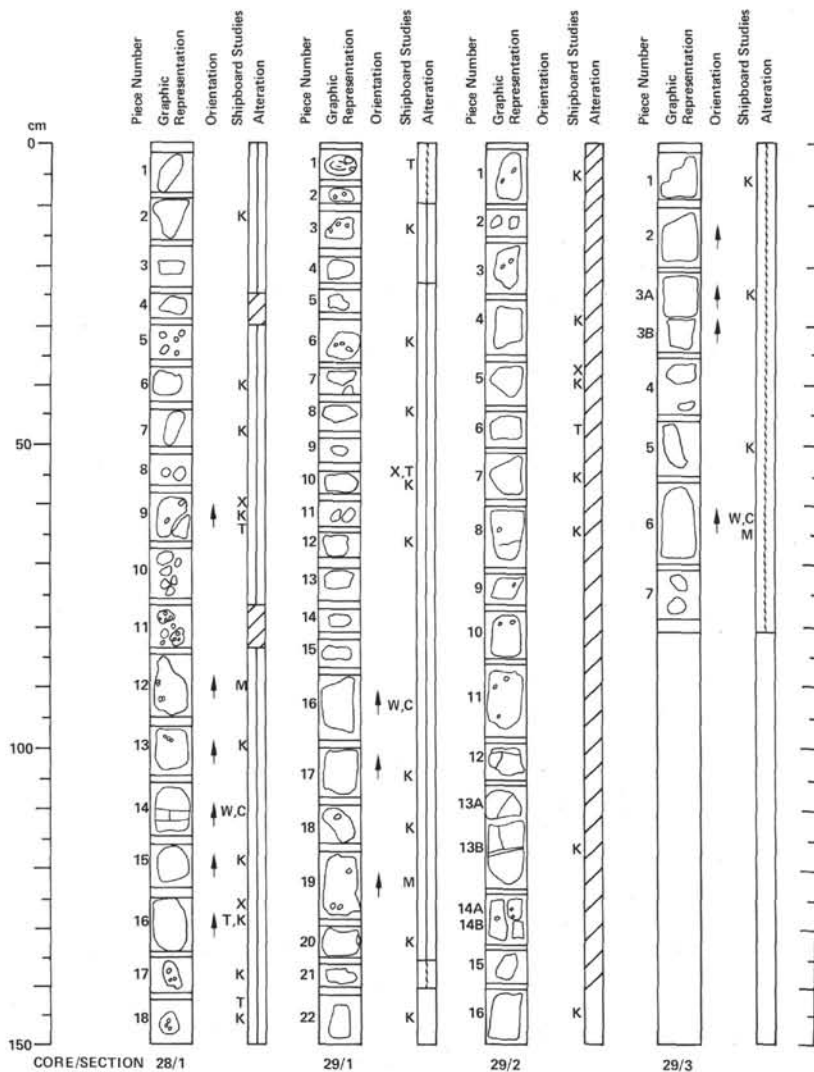
SITE 458		HOLE		CORE 14		CORED INTERVAL: 123.5 to 133.0 m																												
TIME-ROCK UNIT	BIOSTRAT ZONE	FOSSIL CHARACTER		SECTION	METERS	GRAPHIC LITHOLOGY	LITHOLOGIC DESCRIPTION																											
		FORAMS	NANNOS RADS																															
Early Miocene		AP	CM	7	0.5		VOIDS VITRIC SILICEOUS NANNOFOSSIL OOZE with thin beds of SANDY VITRIC ASH Core-Catcher: Similar to Core 11, Section 2, but softer. Dark bands (olive black [5Y 2/1]). Crumbly to soft.																											
				1	1.0																													
				2																														
				3																														
SMEAR SLIDE SUMMARY																																		
<table border="0"> <tr> <td></td> <td>Vitric siliceous nannofossil ooze</td> <td>CC-16</td> <td></td> <td>Sandy vitric ash</td> <td>CC-19</td> </tr> </table>									Vitric siliceous nannofossil ooze	CC-16		Sandy vitric ash	CC-19																					
	Vitric siliceous nannofossil ooze	CC-16		Sandy vitric ash	CC-19																													
TEXTURE:																																		
<table border="0"> <tr> <td>Sand</td> <td>1</td> <td>70</td> </tr> <tr> <td>Silt</td> <td>79</td> <td>29</td> </tr> <tr> <td>Clay</td> <td>20</td> <td>1</td> </tr> </table>								Sand	1	70	Silt	79	29	Clay	20	1																		
Sand	1	70																																
Silt	79	29																																
Clay	20	1																																
TOTAL DETRITAL COMPOSITION:																																		
<table border="0"> <tr> <td>Feldspar</td> <td>3</td> <td>30</td> </tr> <tr> <td>Heavy minerals</td> <td>-</td> <td>5</td> </tr> <tr> <td>Clay</td> <td>15</td> <td>-</td> </tr> <tr> <td>Volcanic glass</td> <td>15</td> <td>65</td> </tr> <tr> <td>Carbonate unsp.</td> <td>5</td> <td>-</td> </tr> <tr> <td>Nannofossils</td> <td>35</td> <td>+</td> </tr> <tr> <td>Diatoms</td> <td>15</td> <td>-</td> </tr> <tr> <td>Radiolarians</td> <td>10</td> <td>-</td> </tr> <tr> <td>Sponge spicules</td> <td>2</td> <td>-</td> </tr> </table>								Feldspar	3	30	Heavy minerals	-	5	Clay	15	-	Volcanic glass	15	65	Carbonate unsp.	5	-	Nannofossils	35	+	Diatoms	15	-	Radiolarians	10	-	Sponge spicules	2	-
Feldspar	3	30																																
Heavy minerals	-	5																																
Clay	15	-																																
Volcanic glass	15	65																																
Carbonate unsp.	5	-																																
Nannofossils	35	+																																
Diatoms	15	-																																
Radiolarians	10	-																																
Sponge spicules	2	-																																

SITE 458		HOLE		CORE 15		CORED INTERVAL: 133.0 to 142.5 m	
TIME-ROCK UNIT	BIOSTRAT ZONE	FOSSIL CHARACTER		SECTION	METERS	GRAPHIC LITHOLOGY	LITHOLOGIC DESCRIPTION
		FORAMS	NANNOS RADS				
Early Miocene		AM	FP	CC	0.5		VITRIC SILICEOUS NANNOFOSSIL OOZE Core-Catcher: Similar to Core 11, Section 2, but mainly olive gray, soft.
				1	1.0		

SITE 458		HOLE		CORE 16		CORED INTERVAL: 142.5 to 152.0 m																			
TIME-ROCK UNIT	BIOSTRAT ZONE	FOSSIL CHARACTER		SECTION	METERS	GRAPHIC LITHOLOGY	LITHOLOGIC DESCRIPTION																		
		FORAMS	NANNOS RADS																						
Early Miocene		RP	RP	0.5	1.0		VITRIC CRYSTAL MUDSTONE and VITRIC MARLY CHALK with thin VITRIC TUFF layers Section 1: Alternating muds, silts, and sands. Sands fine to medium. Silts and muds very strongly burrowed. Some laminations still preserved. No graded bedding. Light olive gray (5Y 6/1), olive gray (5Y 4/1) and dark greenish gray (5GY 4/1). Sands, olive black (5Y 2/1). Section 2: Similar to above but decreasing sand content. Crushed by drilling. Sands lenticular. As marked. Same colors as above, but lighter colors dominant: light olive gray (5Y 6/1) and greenish gray (5GY 6/1). Finer in lower part, possibly more calcareous. Section 3: Light olive gray (5Y 6/1) and greenish gray (5GY 6/1) muds and sandy bands, 5-10 and 12-18 cm: sandy, sand grains scattered through muddy sediments. All strongly burrowed. Core-Catcher: mudstone, strongly burrowed.																		
		RP	B	2																					
		CP	RP	3																					
SMEAR SLIDE SUMMARY																									
<table border="0"> <tr> <td></td> <td>Vitric crystal mudstone</td> <td>1-20</td> <td></td> <td>Vitric marly chalk</td> <td>2-104</td> </tr> </table>									Vitric crystal mudstone	1-20		Vitric marly chalk	2-104												
	Vitric crystal mudstone	1-20		Vitric marly chalk	2-104																				
TEXTURE:																									
<table border="0"> <tr> <td>Sand</td> <td>5</td> <td>-</td> </tr> <tr> <td>Silt</td> <td>10</td> <td>35</td> </tr> <tr> <td>Clay</td> <td>85</td> <td>65</td> </tr> </table>								Sand	5	-	Silt	10	35	Clay	85	65									
Sand	5	-																							
Silt	10	35																							
Clay	85	65																							
TOTAL DETRITAL COMPOSITION:																									
<table border="0"> <tr> <td>Feldspar</td> <td>25</td> <td>-</td> </tr> <tr> <td>Heavy minerals</td> <td>1</td> <td>-</td> </tr> <tr> <td>Clay</td> <td>64</td> <td>40</td> </tr> <tr> <td>Volcanic glass</td> <td>10</td> <td>30</td> </tr> <tr> <td>Carbonate unsp.</td> <td>-</td> <td>20</td> </tr> <tr> <td>Nannofossils</td> <td>-</td> <td>10</td> </tr> </table>								Feldspar	25	-	Heavy minerals	1	-	Clay	64	40	Volcanic glass	10	30	Carbonate unsp.	-	20	Nannofossils	-	10
Feldspar	25	-																							
Heavy minerals	1	-																							
Clay	64	40																							
Volcanic glass	10	30																							
Carbonate unsp.	-	20																							
Nannofossils	-	10																							
Remarks: Sudden change in lithification semi-lithified fragments alternating with crushed sediments.																									

SITE 458		HOLE		CORE 17		CORED INTERVAL: 152.0 to 161.5 m	
TIME-ROCK UNIT	BIOSTRAT ZONE	FOSSIL CHARACTER		SECTION	METERS	GRAPHIC LITHOLOGY	LITHOLOGIC DESCRIPTION
		FORAMS	NANNOS RADS				
Early Miocene		AP	RP	CC	0.5		VITRIC MARLY CHALK Section 1 is olive black sand, very fine, greenish gray (5GY 6/1) and silty mudstone strongly burrowed, light gray (N7). Core-Catcher: Bits of mudstone as above.
				1	1.0		





60-458-28 3705.5-3715.0 m (256.5-266.0 m, BSF)

High-Mg bronzite andesite

Moderately to intensely altered brown to brownish-gray high-Mg aphyric bronzite andesite. Relict glass present on Pieces 3, 6, and 7. Several others have a spherulitic appearance. Vesicles comprise up to 20% of some pieces, but are very small (1 mm or less). Probable pillowed sequence.

Thin Section Description

28-1, 9-13 cm. Hyalopilitic bronzite andesite. Microphenocrysts of clinopyroxene (~6%) and opx (~1%) are set in a glassy groundmass crowded with clinopyroxene microlites. Most opx phenocrysts are intergrown with cpx. Plagioclase is absent except for possible needles in brown spherulites. Alteration minor to clays around vesicles, plus some zeolites in vesicles. Vesicles are tiny, and about 40% of the rock. No Fe-Ti oxides.

28-1, 64-67 cm. Hyalopilitic intersertal bronzite andesite. Rock has 1-2% cpx phenos, and up to 50% tiny vesicles (0.5-1 mm; irregular shape). The remaining groundmass is about equally divided between glass (partially altered) and prismatic to skeletal cpx.

28-1, 111-114 cm. Intersertal to spherulitic bronzite andesite. Rock has ~4% cpx and ~1% opx phenocrysts, some with irregular blocky twinning, others which appear strained (do not go entirely to extinction). The groundmass is about 50% vesicles, 20% cpx microlites, and 10% skeletal plagioclase. Alteration is minor (clays and zeolites).

28-1, 130-133 cm. Spherulitic bronzite andesite. Rock has ~5% cpx phenocrysts set in a groundmass of about 45% vesicles (0.5-1 mm, irregular shape, lined with clays), ~10% plagioclase (skeletal to acicular), ~7% cpx (chunky to prismatic), ~40% brown devitrified glass, and traces of opaque minerals (partly oxidized).

28-1, 142-146 cm. Hyalopilitic bronzite andesite. Rock has 10% tabular, anhedral, and interpenetrative clinopyroxene phenocrysts, and ~2% opx phenocrysts rimmed with cpx. Groundmass has ~10% round to irregular scattered vesicles 0.2-2 mm in diameter, 35% euhedral to prismatic, flow textured cpx microlites, 2% plagioclase needles, 3% euhedral to prismatic opx phenocrysts, and 38% clear glass.

	J _{NRM}	MDF	Inc.	S	D	Rock Type
28-1, 90-92 cm	0.957x10 ⁻³	185	+34.4	---	---	---
28-1, 110-112 cm	---	---	---	3.79	2.26	Alt. High-Mg andesite

60-458-29 3715.0-3724.5 m (266.0-275.5 m, BSF)

High-Mg bronzite andesite

Continuation of pillowed sequence in Core 28. Brown, gray-brown, and gray aphyric high-Mg bronzite andesite. Alteration more intense than in Core 28. Relict glass was not recovered in this core, but several pieces are spherulitic, indicating that this was a sequence of small pillows or possibly thin flows. More massive, holocrystalline rocks were recovered in Sections 2 and 3. Vesicles make up 5-15% of the rocks, and in some cases are elongate. Most are tiny (pin-hole size), but a few are up to 2 cm long. Cracks and veins filled with secondary minerals (calcite and smectite) are abundant.

Thin Section Descriptions

29-1, 1-3 cm. Intersertal to hyalopilitic bronzite andesite. Rock has about 4% cpx and 1% opx (bronzite) phenocrysts set in a groundmass of 40% vesicles, 30% acicular clinopyroxene microlites, and 19% glass. Alteration is minor (clays lining vesicles, zeolite ? in glass).

29-1, 54-57 cm. Variolitic bronzite andesite. Rock has about 3% euhedral to tabular cpx phenocrysts up to 1 mm set in groundmass of ~20% irregular vesicles (up to 1 mm), 35% plagioclase, 10% cpx, 4% magnetite, and 15% devitrified glass. About 10% clays line vesicles and replace glass.

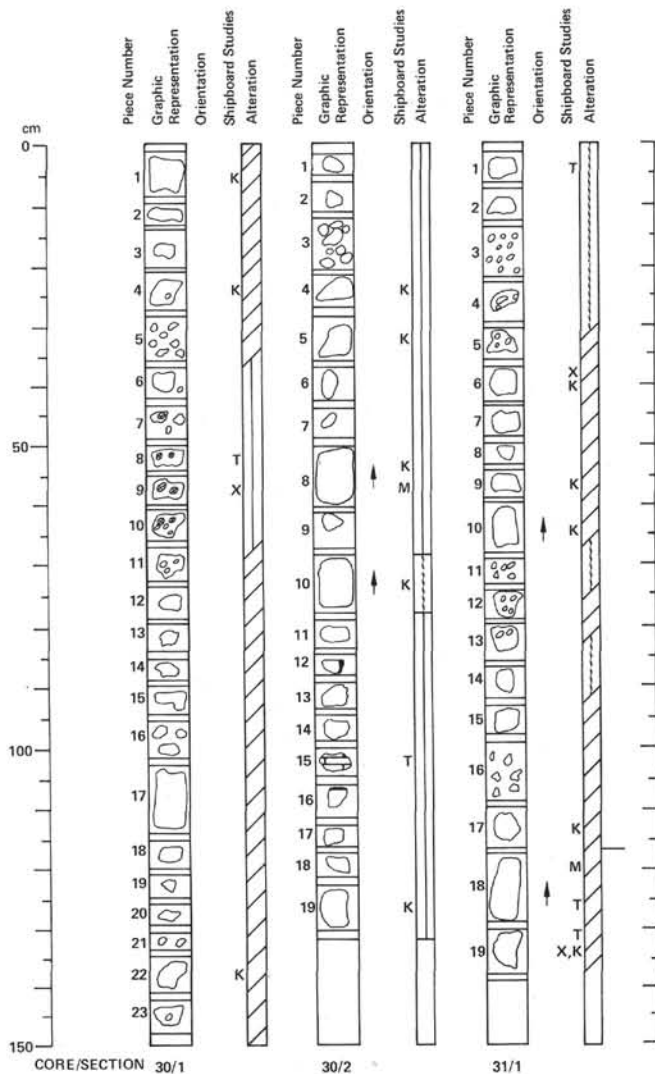
29-1, 92-95 cm. Essentially identical to 29-1, 54-57 cm except it has about 40% vesicles, ~15% clays and a trace of zeolites.

29-2, 39-42 cm. Intersertal bronzite andesite. Rock has only very rare cpx phenocrysts set in a groundmass of 40% vesicles (2.0-0.5 mm); irregular shape, ~20% skeletal plagioclase, ~15% cpx crystals, ~5% euhedral opx crystals, and about 20% altered glass (to green and brown clays).

29-2, 38-40 cm. From nearly the same interval as the previous thin section. Rock is very similar except it has only 10% vesicles, and more altered glass (~35-40%).

29-2, 48-49 cm. Intersertal bronzite andesite. Rare cpx phenocrysts are set in a groundmass of ~20% vesicles (0.5-1 mm, irregular shape), ~25% skeletal plagioclase, ~20% granular to dendritic clinopyroxene, ~5% blocky orthopyroxene, a trace of opaque minerals and perhaps of quartz, and ~30% clay minerals after glass.

	J _{NRM}	MDF	Inc.	S	D	Rock Type
29-1, 93-95 cm	---	---	---	3.17	2.19	Alt. High-Mg andesite
29-1, 121-124 cm	2.21x10 ⁻³	211	+37.8	---	---	---
29-2, 82-84 cm	---	---	---	3.25	2.09	Alt. High-Mg andesite
29-2, 92-94 cm	0.579x10 ⁻³	221	+35.3	---	---	---
29-3, 60-62 cm	---	---	---	3.15	2.15	Alt. High-Mg andesite
29-3, 64-66 cm	1.18x10 ⁻³	225	+33.1	---	---	---



60-458-30 3724.5-3734.0 m (275.5-285.0 m, BSF)

High-Mg bronzite andesite

Aphyric, fine- to medium-grained, gray to greenish-gray moderately to intensely altered high-Mg bronzite andesite. Pieces are probable pillow fragments. Section 1, Pieces 7-10, and Section 2, Pieces 12, 13, and 16-18 are spherulitic, with traces of former glassy margins. Vesicles are 2.5 mm, make up to 15% of the rocks, and locally are arranged in streaks. A fragment of limestone with a piece of andesite attached was recovered in Section 2 (Piece 15). Rocks are partially altered to clay minerals along fractures, and quartz or chalcedony fills some amygdules (Pieces 7-10, Section 1).

Thin Section Descriptions

30-1, 50-54 cm. Hyalopilitic bronzite andesite with incipient variolites. About 2% skeletal to dendritic clinopyroxene phenocrysts (up to 0.5 mm) and a trace of orthopyroxene phenocrysts (enclosed by cpx) are set in a groundmass of 40% acicular clinopyroxene microlites, 55% glass and 5% rounded vesicles. Some of the glass is altered to zeolite. Plagioclase and opaque minerals are absent.

30-1, 100-104 cm. Hyalopilitic bronzite andesite. The rock contains a trace of orthopyroxene microphenocrysts (0.5-1 mm) set in a groundmass of about 30% acicular clinopyroxene, 5% irregular or flattened vesicles lined with zeolite, and 64% glass (mostly altered to clays).

30-2, 71-73 cm. Intersertal bronzite andesite. The rock contains a trace of clinopyroxene microphenocrysts (~1 mm) set in a groundmass of about 50% vesicles (0.3-1 mm), 25% plagioclase, 10-13% clinopyroxene, 1-2% opx, 5-10% glass (altered to clays), and a trace of opaques.

30-2, 100-104 cm. Limestone with glass fragments. Glass has about 10% cpx microlites and 15% plagioclase needles in a spherulitic morphology, plus about 50% vesicles. Clays line the vesicles.

	J_{NRM}	MDF	Inc.	S	D	Rock Type
30-1, 105-107 cm	1.51×10^{-3}	261	+13.5	—	—	—
30-1, 110-112 cm	—	—	—	3.21	2.23	Alt. High-Mg andesite
30-2, 56-58 cm	1.25×10^{-3}	257	+14.9	—	—	—
30-2, 71-73 cm	—	—	—	3.16	2.06	Alt. High-Mg andesite

60-458-31 3734.0-3743.5 m (285.0-294.5 m, BSF)

High-Mg bronzite andesite

A transition between the upper pillowed sequence (lithologic unit 1) and two more massive flows to high-Mg bronzite andesite (lithologic unit 2) is between Pieces 17 and 18. Pieces 1-17 are fragments of pillows or thin flows, fine- to medium-grained, generally vesicular, with vesicles up to 3.5 mm diameter. Alteration is moderate to intense, mainly to clay minerals. Pieces 1-4, 11 and 14 are highly altered, and amygdaloidal, with chalcedony(?) in amygdules. The color is light olive gray to grayish-green.

Thin Section Descriptions

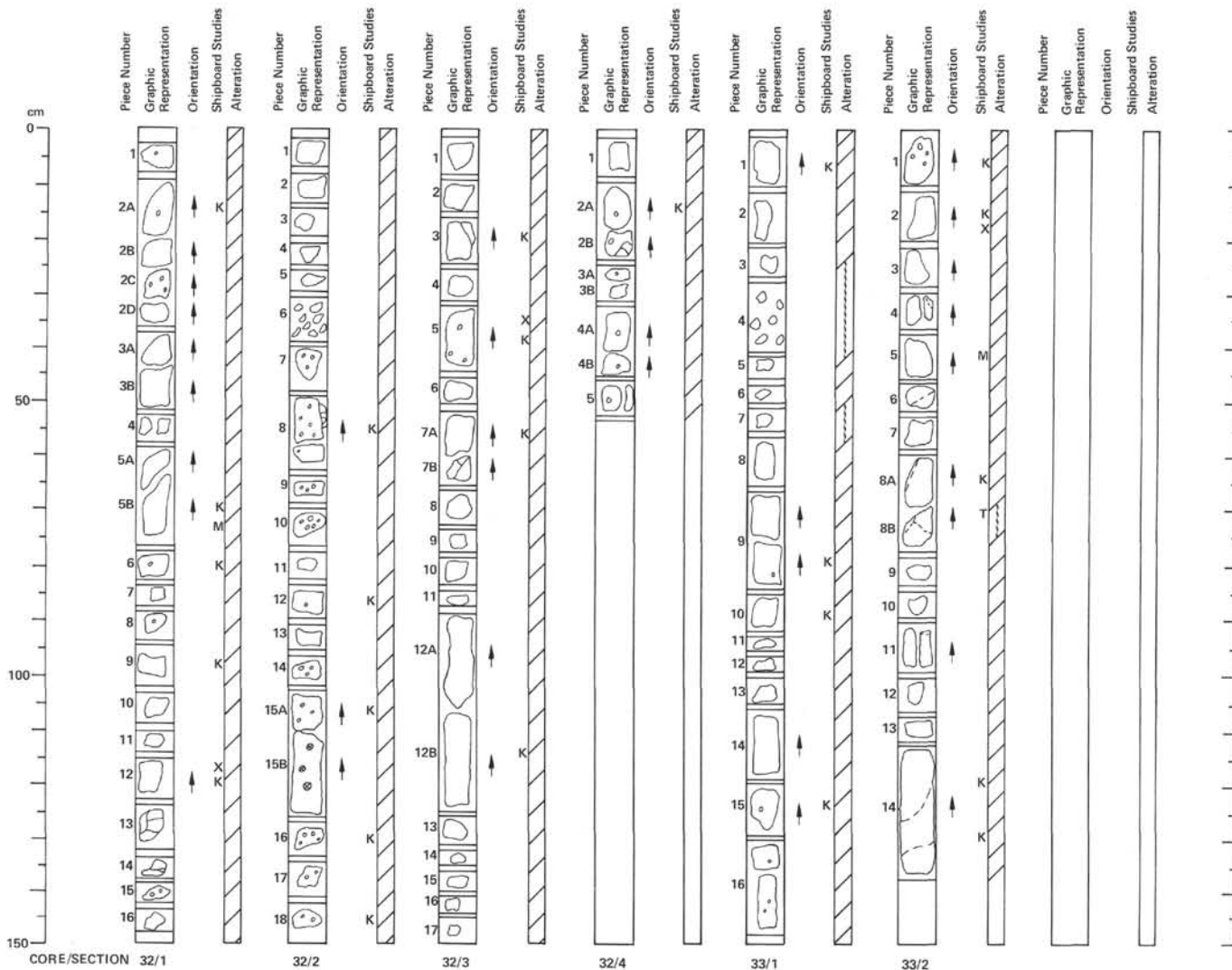
31-1, 2-7 cm. Generally subophitic bronzite andesite with local intersertal patches. The rock lacks phenocrysts and consists of subequal proportions of plagioclase (An_{76-60}), clinopyroxene, and devitrified glass with lesser orthopyroxene (2%), and a trace of opaque minerals. Clays replace about half the glass, and vesicles are about 10% of the rock.

31-1, 127-129 cm. Subophitic bronzite andesite with local intersertal patches. Very similar to 31-1, 2-7 cm, but about twice as vesicular.

31-1, 130-131 cm. Subophitic bronzite andesite, with about 40% plagioclase, 30% clinopyroxene, 15% altered glass, and 1-2% orthopyroxene. Vesicles make up about 12% of the rock.

31-1, 130-135 cm. Sample taken from near a large vesicle. Texture ranges from spherulitic to subophitic within the thin section. Same mineralogy as 31-1, 130-131 cm, and about the same vesicularity.

	J_{NRM}	MDF	Inc.	S	D	Rock Type
31-1, 121-123 cm	0.656×10^{-3}	178	+34.5	—	—	—
31-1, 125-128 cm	—	—	—	3.84	2.43	Alt. High-Mg andesite



60-458-32 3743.5-3753.0 m (294.5-304.0 m, BSF)

High-Mg bronze andesite
 Continuation of the massive flow recovered in the lower part of Core 31. Fine- to medium-grained, aphyric, greenish-gray (5G 6/1) to dark greenish-gray (5GY 4/1), generally fresh, but with veins of carbonate, green smectite, and perhaps chlorite. Some exterior surfaces are coated with these minerals. Most pieces are slightly vesicular (0.1-1.0 mm). Vesicles may be filled with zeolite in Sections 2-4.

Thin Section Descriptions
32-1, 81-83 cm. Subophitic bronze andesite. The rock has no phenocrysts and consists of a groundmass with about 15% devitrified and altered glass, 10% vesicles and the remainder about equally divided between plagioclase and clinopyroxene. Orthopyroxene and opaque minerals each are about 1%.
32-2, 64-66 cm. Subophitic to intersertal bronze andesite. The rock has no phenocrysts and consists of groundmass with about 35% plagioclase, 25% clinopyroxene, and 2% opaque minerals. Vesicles make up about 20% of the groundmass, and alteration minerals the remainder (10% carbonate on an exterior surface, 10% clays lining vesicles and replacing glass, and 3% zeolites replacing clays).
32-2, 123-125 cm. Intersertal to subophitic bronze andesite. The rock contains a trace of clinopyroxene microphenocrysts, set in a groundmass of about 30% acicular to tabular plagioclase, 20% equant to tabular clinopyroxene, 1-2% opaques, and 8% irregular to ovoid vesicles (0.1-1 mm). The remainder is altered glass (minor carbonate, mostly clays, some zeolites).
32-3, 113-117 cm. Intersertal bronze andesite. The rock has no phenocrysts, and consists of about 30% plagioclase, 10% clinopyroxene, 3-4% opaque minerals, 5% glass, 30% irregular to ovoid vesicles, and 22% secondary minerals (mostly clays, but with about 2% zeolites lining vesicles).
32-4, 40-42 cm. Intersertal to subophitic bronze andesite. The rock has no phenocrysts, and consists of about equal proportions of acicular to tabular plagioclase, and equant to tabular clinopyroxene, with lesser devitrified glass and traces of opaques. There are about 15% irregular to ovoid vesicles, 20% interstitial clay, and 2% zeolites after glass.

	J _{NRM}	MDF	Inc.	S	D	Rock Type
32-1, 48-50 cm	---	---	---	3.98	2.44	Alt. High-Mg andesite
32-1, 72-74 cm	0.630x10 ⁻³	197	+34.5	---	---	---
32-2, 118-120 cm	0.465x10 ⁻³	138	+31.8	---	---	---
32-3, 112-117 cm	---	---	---	4.36	---	Alt. High-Mg andesite
32-3, 119-121 cm	3.31x10 ⁻³	151	+31.3	---	---	---

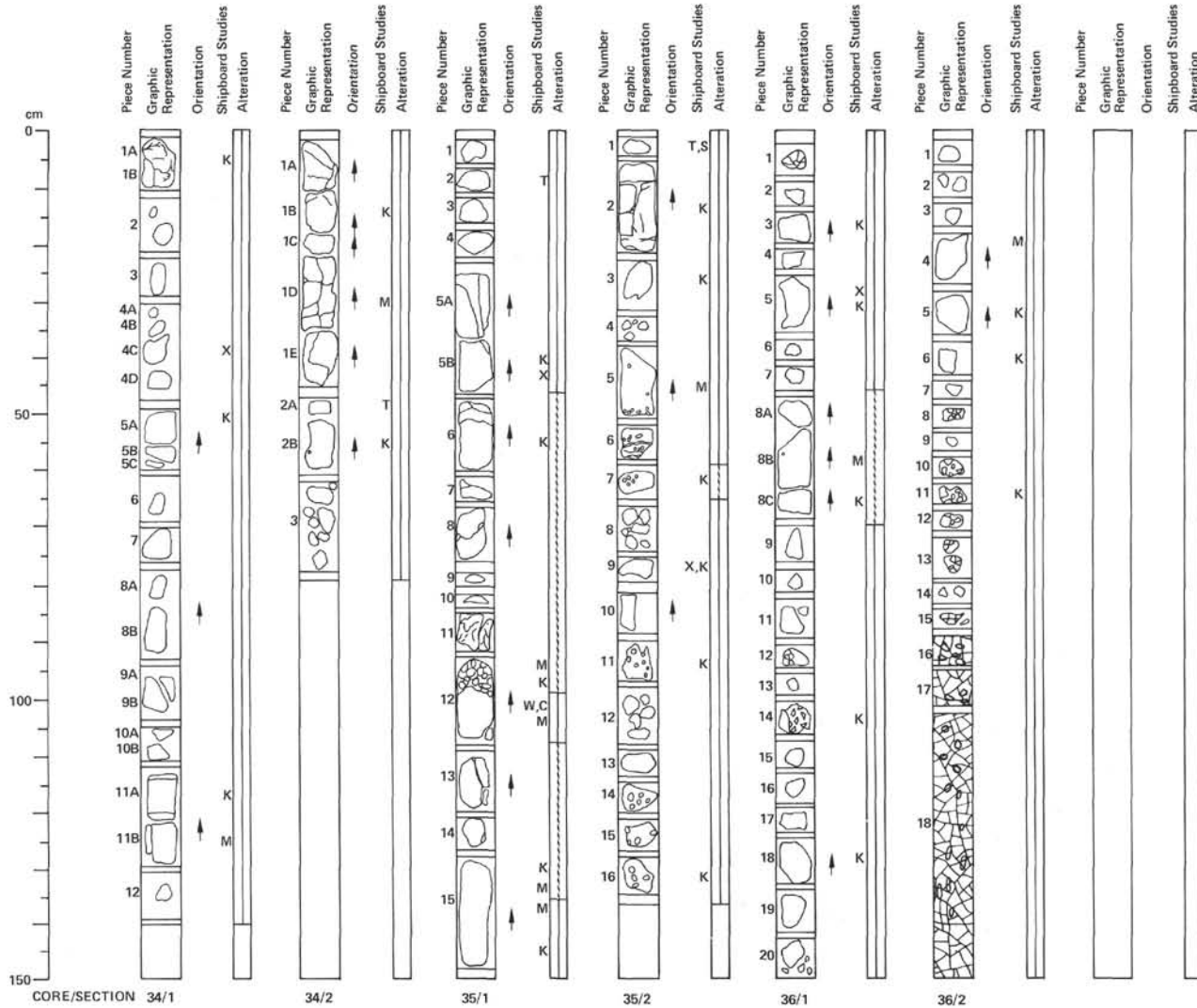
60-458-33 3753.0-3762.5 m (304.0-313.5 m, BSF)

High-Mg bronze andesite
 Medium- to coarse-grained slightly vesicular high-Mg bronze andesite, medium gray in color and almost holocrystalline. Pieces are moderately to intensely altered. Interstitial groundmass partially altered to brown clay. Veins are lined with carbonate and clay minerals. Section 2, Piece 1 has a large elongate vesicle (up to 15 mm long). Irregular cracks are filled with carbonate and opaline silica in Section 2, Pieces 4, 8, 11, and 14. Greenish-gray and greenish-black clay minerals also occur. The small pieces of Section 1, 28-40 cm are highly altered with obvious foliation or slickensides, and have a soapy feel.

Thin Section Descriptions
33-1, 58-60 cm. Subophitic high-Mg andesite. The rock lacks phenocrysts and consists of about 60% plagioclase, 20% clinopyroxene, 10% vesicles, traces of opaques, and about 5% mesostasis (with 2-3% clays). Plagioclase is euhedral and tabular or patchy and interstitial. The rock contains about 2% quartz.
33-2, 70-72 cm. Subophitic bronze andesite. Coarsest grained rock at Site 458. The rock lacks phenocrysts, and is about equal proportions of clinopyroxene and plagioclase with about 1% opaques and a trace of orthopyroxene. The rock has about 10% vesicles (0.1-1 mm, irregular shape, scattered), and 15% altered mesostasis. A thin carbonate vein goes through the section.

	J _{NRM}	MDF	Inc.	S	D	Rock Type
33-1, 112-115 cm	---	---	---	4.71	2.63	Alt. High-Mg andesite
33-1, 115-117 cm	0.708x10 ⁻³	228+	+35.9	---	---	---
33-2, 42-44 cm	0.988x10 ⁻³	252	+34.0	---	---	---
33-2, 63-68 cm	---	---	---	4.25	---	High-Mg andesite

SITE 458



60-458-34 3762.5-3772.0 (313.5-323.0 m, BSF)

High-Mg bronzite andesite

A continuation of the massive material beginning in Core 32. Moderately to intensely altered medium-grained greenish-gray bronzite andesite. Rocks are aphyric, with > 10% small spherical and/or irregular vesicles. They are variably veined and fractured, with secondary clays and carbonate on fracture surfaces, and in veins and amygdules.

Thin Section Description

34-2, 48-52 cm. Subophitic bronzite andesite. The rock is dominated by plagioclase (~40%), with lesser clinopyroxene (~23%), vesicles (~20%), clay minerals (~10%) and traces of opaques, quartz(?), secondary carbonate, and zeolites.

	J _{NRM}	MDF	Inc.	S	D	Rock Type
34-1, 113-118 cm	—	—	—	4.23	—	Ves. andesite
34-1, 123-125 cm	1.83×10^{-3}	168	+29.9	—	—	—
34-2, 30-32 cm	0.479×10^{-3}	204	+34.7	—	—	—

60-458-35 3772.0-3781.5 m (323.0-332.5 m, BSF)

High-Mg bronzite andesite

A continuation of the massive flow which began in Core 32, plus the top of another flow in Section 2. The rocks are moderately to intensely altered, aphyric, variably veined and fractured, fine- to medium-grained high-Mg bronzite andesite. Carbonate veins are shot through most of the fragments. An apparent type of cemented fracture breccia was recovered in Section 1, Pieces 12 and 15. Rounded fragments occur in a fracture matrix in these pieces. Pieces in Section 2 tend to be much more vesicular than in Section 1. Vesicles comprise 15-20% of some pieces and are large (up to 13 mm) in the lower part of the section. Clay mineral alteration (veins and as groundmass replacement) is also more prominent in Section 2.

Thin Section Descriptions

35-1, 8-10 cm. Subophitic bronzite andesite. The rock lacks phenocrysts, and consists of about 30% plagioclase microlites, 20% clinopyroxene, minor opaques, a trace of quartz(?), and 20% scattered, irregularly shaped vesicles. The remainder is a microcrystalline once-glassy mesostasis, altered to clays. A minor carbonate vein crosses a portion of the section.

35-2, 69-71 cm. Spherulitic, altered, clinopyroxene-rich high-Mg andesite. The rock consists of about 10% clinopyroxene microlites and spherulites set in glass, now altered to clays. There are about 5% vesicles (scattered, round, 0.05-1 mm).

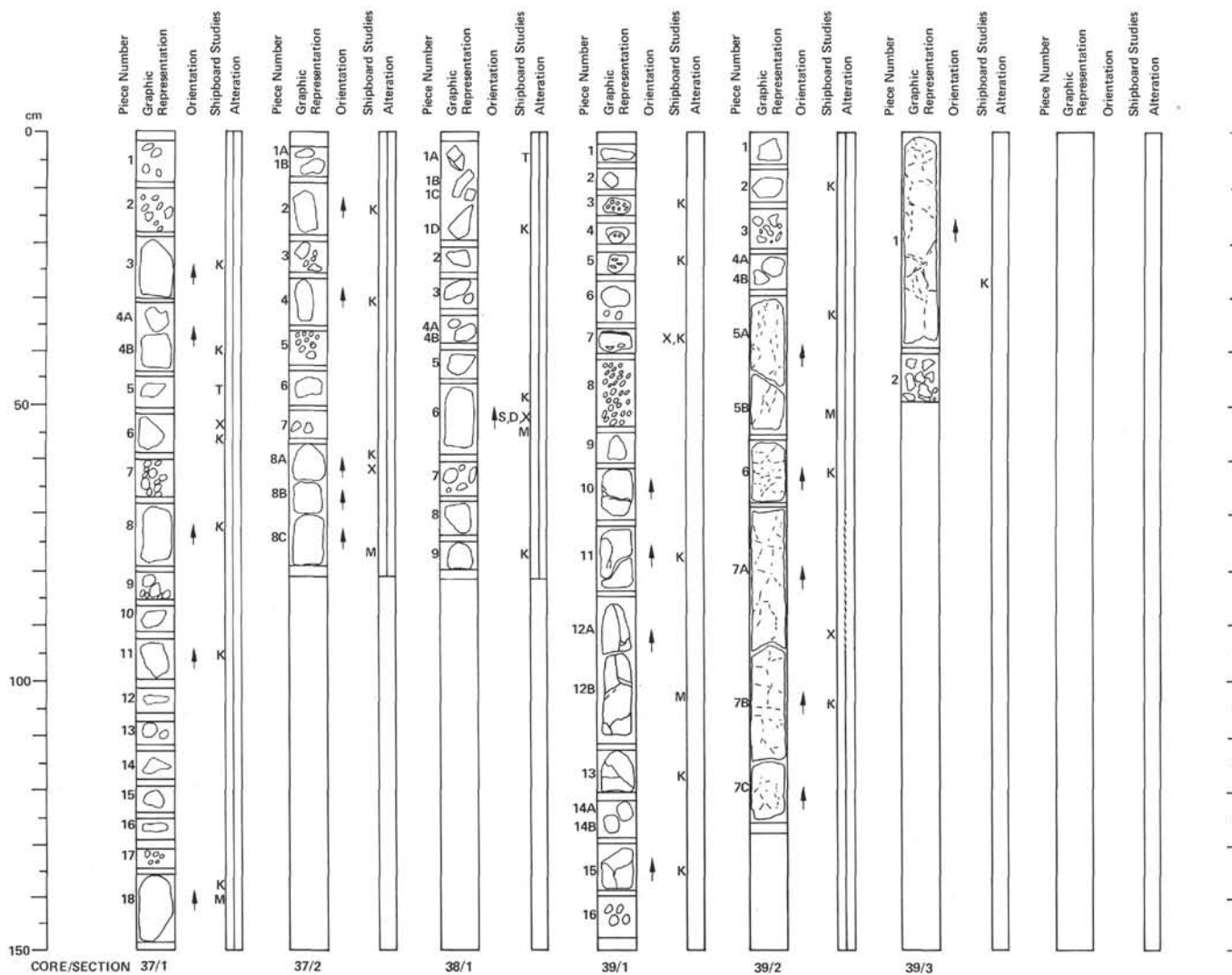
	J _{NRM}	MDF	Inc.	S	D	Rock Type
35-1, 97-99 cm	0.183×10^{-3}	152+	+58.2	—	—	—
35-1, 100-102 cm	—	—	—	3.84	—	Ves. andesite
35-1, 103-105 cm	0.468×10^{-3}	189+	+28.4	—	—	—
35-1, 133-135 cm	0.313×10^{-3}	179+	+7.5	—	—	—
35-1, 137-139 cm	0.892×10^{-3}	183+	+34.5	—	—	—
35-2, 43-45 cm	—	—	—	3.36	2.17	Ves. andesite
35-2, 46-48 cm	2.12×10^{-3}	242	+28.2	—	—	—

60-458-36 3781.5-3791.0 m (332.5-342.0 m, BSF)

High-Mg bronzite andesite

A continuation of the fairly massive flow material begun in Core 32. The rocks are fine- to medium-grained dark greenish-gray, moderately to intensely altered high-Mg bronzite andesite. The rocks become very intensely fractured, even mylonitized, downward. Cemented fracture breccias occur in both sections (Section 1, Piece 14; Section 2, Pieces 8 and 10-13). Slickensides occur on the larger pieces (1-6) of Section 2. In the fracture breccias and mylonite zones, clay-mineral alteration is intense. A magnetic transition occurs just above the zone of intense mylonitization.

	J _{NRM}	MDF	Inc.	S	D	Rock Type
36-1, 55-57 cm	1.59×10^{-3}	280	+32.5	—	—	—
36-1, 58-60 cm	—	—	—	3.26	2.23	Ves. andesite
36-2, 22-24 cm	0.799×10^{-3}	310	+18.4	—	—	—



60-458-37 3791.0-3800.5 m (342.0-351.5 m, BSF)

High-Mg bronzite andesite

A continuation of the fairly massive flow material begun in Core 32. The rocks are not as fractured as in Core 36. They are fairly intensely altered, aphyric olive gray to medium gray high-Mg bronzite andesites. The larger pieces tend to be fracture-free, but the intervals where nothing but pebbles were recovered probably represent fractured zones in the hole. The core is the base of the second massive flow in lithologic unit 2.

Thin Section Description

37-1, 45-47 cm. Intersertal to spherulitic bronzite andesite. The rock lacks phenocrysts, and consists of about 30% plagioclase, 15% clinopyroxene, 1% orthopyroxene, and a trace of opaque minerals. Vesicles are about 5% (0.1-1.0 mm, scattered, irregular shape). The rest of the rock is a microcrystalline glassy mesostasis with abundant tiny plagioclase and clinopyroxene crystallites, now largely altered to clays.

	J_{NRM}	MDF	Inc.	S	D	Rock Type
37-1, 72-76 cm	---	---	---	3.80	---	Ves. andesite
37-1, 142-144 cm	3.36×10^{-3}	183	+23.3	---	---	---
37-2, 77-79 cm	5.64×10^{-3}	279	+21.0	---	---	---

60-458-38 3800.5-3810.0 m (351.5-361.0 m, BSF)

High-Mg bronzite andesite

Altered aphyric high-Mg bronzite andesite, slightly vesicular (10%), no veins, few fractures, medium bluish-gray (5B 5/1) to greenish-gray (5GY 6/1). Rocks are fine-grained to very fine-grained.

Thin Section Description

38-1, 5-7 cm. Hyalopilitic, somewhat pilotaxitic high-Mg andesite. The rock has about 5% microphenocrysts of clinopyroxene (skeletal, dendritic, prismatic), and 1% orthopyroxene (prismatic, $2V = 80-85^\circ$ - "bronzite"), set in a groundmass with 35% clinopyroxene microlites and an altered, once completely glassy mesostasis. The rock shows zoned alteration, with clays and Fe-hydroxides on the outside, and clear, faintly birefringent zeolite replacing glass on the inside. There are about 5% vesicles, all rounded, mainly on one side of the piece.

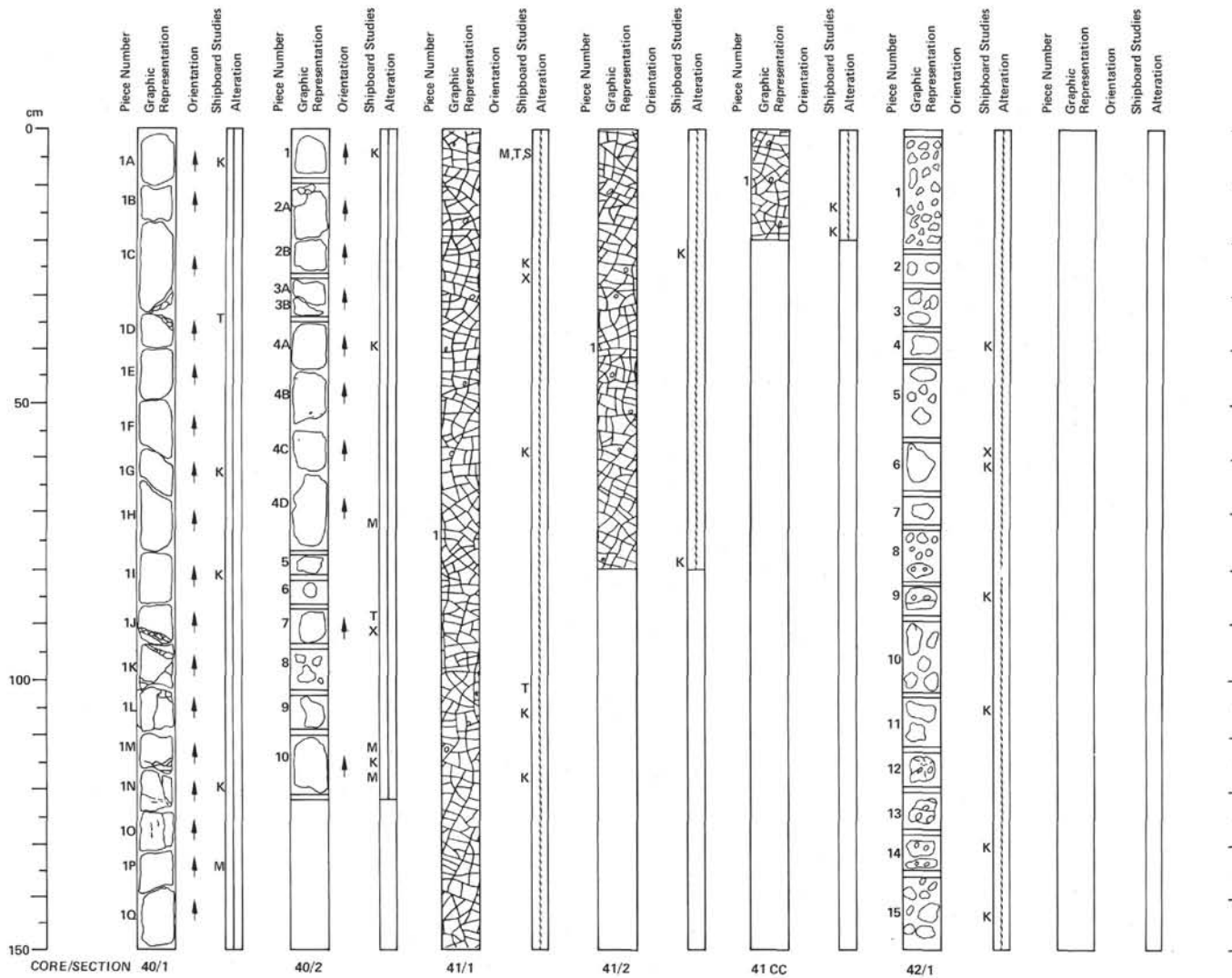
	J_{NRM}	MDF	Inc.	S	D	Rock Type
38-1, 49-53 cm	---	---	---	3.85	---	Ves. andesite
38-1, 55-57 cm	0.894×10^{-3}	169	+19.3	---	---	---

60-458-39 3810.0-3819.5 m (361.0-370.5 m, BSF)

High-Mg bronzite andesite

Moderately to intensely altered aphyric high-Mg bronzite andesite, with varying degrees of vesicularity, generally olive gray in color. Section 1, Piece 7 has a flat, upper glassy and spherulitic margin. Section 1, Pieces 9-16 are highly fractured, and have clays filling the fractures. Material in Sections 2 and 3 was more coherently recovered, but was riddled with a complex network of cracks and fractures, cemented by a greenish-black clay minerals. Nearer the cracks, alteration is more intense, with a dark greenish-gray color. Elsewhere, the rock is fresher, and bluish-gray in color. Lower in the core, a whitish clay mineral also partially fills cracks, and in Section 3, native copper lines several veins.

	J_{NRM}	MDF	Inc.	S	D	Rock Type
39-1, 102-108 cm	---	---	---	3.24	---	Ves. andesite
39-1, 106-108 cm	1.17×10^{-3}	306	+37.5	---	---	---
39-2, 51-53 cm	0.776×10^{-3}	268	+35.1	---	---	---
39-2, 60-62 cm	---	---	---	3.56	2.28	Ves. andesite
39-3, 15-17 cm	0.529×10^{-3}	253	+35.7	---	---	---



60-458-40 3819.5-3829.0 m (370.5-380.0 m, BSF)

High-Mg bronze andesite

The material in this core resembles that in Core 39 in that it is fairly massive, fine-grained, and dark greenish gray, with an irregular network of cracks, filled with greenish-black and greenish-gray clay minerals, and possibly a white zeolite. Altered and fractured zones in Section 1 between Pieces 1C, 1D, and 1J, 1K look like inter-pillow hyaloclastite zones. There is no visible native copper. Pieces in Section 2 are a bit more vesicular than in Section 1. This core represents the base of the upper high-Mg bronze andesite (chemical unit A₁).

Thin Section Descriptions

40-1, 33-35 cm. Altered hyalopilitic high-Mg andesite. There are about 3% skeletal to prismatic clinopyroxene microphenocrysts up to 0.5 mm (altered), set in a groundmass with about 40% vesicles (0.1-0.5 mm), 10% microlitic clinopyroxenes, and the remainder altered mesostasis. The mesostasis is now clays, but has a streaky appearance produced by flow.

40-2, 88-90 cm. Intersertal high-Mg andesite with about 5% skeletal clinopyroxene microphenocrysts (0.2-0.7 mm), set in a groundmass with about 5% clinopyroxene microlites (0.1-0.2 mm) arranged in spherulitic swarms. Many are skeletal and altered to clays. The rock originally contained about 40% vesicles. Most of the rock is now clays.

	J-NRM	MDF	Inc.	S	D	Rock Type
40-1, 79-85 cm	—	—	—	3.01	—	Ves. andesite
40-1, 134-137 cm	1.34x10 ⁻³	264	+34.7	—	—	—
40-2, 72-75 cm	1.64x10 ⁻³	364	+38.0	—	—	—
40-2, 115-117 cm	1.07x10 ⁻³	381	+40.2	—	—	—

60-458-41 3829.0-3838.5 m (380.0-389.5 m, BSF)

Aphyric basalt

Fine- to medium-grained, aphyric, very intensely altered, highly fractured, slightly vesicular basalt. Color is darker than in high-Mg bronze andesites of Cores 29-40. Here it is greenish-black (5G 2/1). Both sections are fractured into angular fragments ranging in size from millimeters to 5-10 cm. Fracturing is partly related to drilling, though most of it must have been along pre-existing cracks. A greenish-gray micaceous mineral is pervasively distributed through the core, particularly along incipient fractures.

Thin Section Descriptions

41-1, 3-5 cm. Intersertal basalt with traces of plagioclase and clinopyroxene microphenocrysts. The rock contains about 15% vesicles up to 5 mm in diameter, 25% plagioclase microlites, 3-5% skeletal to microlitic clinopyroxene, and 2-3% titanomagnetite. The rest is mesostasis divided between brown oxidized glass and pale green clays. Brown is most abundant near interconnected vesicles. Cpx has largely been replaced by clays.

41-1, 22-26 cm. Intersertal basalt with traces of plagioclase and clinopyroxene microphenocrysts. The rock is very similar to 41-1, 3-5 cm in mineralogy, but appears more altered. Darker, more spherulitic zones occur near vesicles.

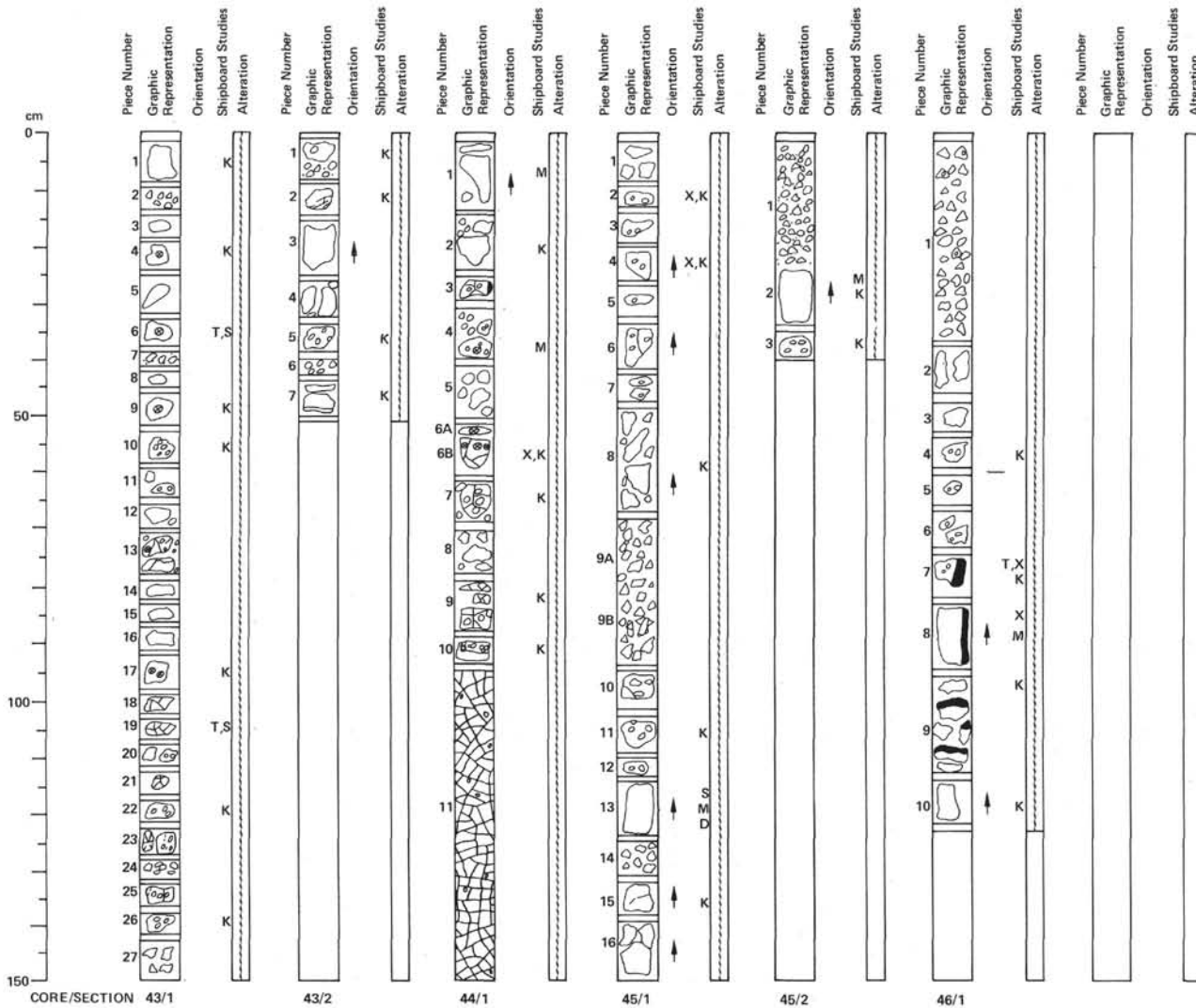
	J-NRM	MDF	Inc.	S	D	Rock Type
41-1, 3-5 cm	2.68x10 ⁻³	213	-15.6	—	—	—
41-1, 122-124 cm	—	—	—	2.83	2.13	Basalt

60-458-42 3838.5-3848.0 m (389.5-399.0 m, BSF)

High-Mg bronze andesite

Intensely to very intensely altered, fine- to medium-grained, dark greenish gray (5G 4/1) to greenish-black (5G 2/1) high-Mg bronze andesite. Pervasively altered to clay minerals, and possibly chlorite, zeolite, and a silica mineral. Most fragments appear to be parts of pillows. Vesicular pieces (vesicles 0.2-4 mm) are generally more altered than massive passive. Vesicles are filled with above secondary minerals. Vesicular pieces also tend to be laced with veins of secondary minerals.

	J-NRM	MDF	Inc.	S	D	Rock Type
42-1, 133-136 cm	—	—	—	5.08	—	Ves. basalt



60-458-43 3848.0-3857.5 m (399.0-408.5 m, BSF)

High-Mg bronzite andesite

Fine-grained, aphyric, greenish-black (5GY 2/1) to dark greenish-gray (5G 4/1) high-Mg bronzite andesite, riddled with veins and fractures. Two types of fragments can be distinguished: 1) massive very fine-grained sparsely vesicular to non-vesicular, dark greenish-gray pieces with fractures (very thin and probably very closely spaced), lined with zeolite (phillipsite?) and green smectite (nontronite?). Alteration is generally penetrative; 2) vesicular (0.2-2.5 mm), greenish-black aphyric, variolitic, highly fractured (fractures up to 2 mm wide) filled with zeolite (phillipsite?) and green smectite (nontronite?), apparently without carbonate. Type 2 apparently represents pillow rind fragments whereas type 1 could represent pillow interior fragments.

Thin Section Descriptions

43-1, 34-37 cm. Spherulitic high-Mg andesite, very badly altered. There are abundant swarms of spherulitic plagioclase and minor skeletal clinopyroxene. Glass between spherulite fibers is now shot to clays. Clinopyroxene crystallized before plagioclase. Plag: cpx relative abundances quite different from Core 41 thin sections. Clays are ubiquitous.

43-1, 104-107 cm. Intersertal high-Mg andesite. The rock is aphyric, but has about 50% skeletal to euhedral plagioclase (An₅₅ g), 5% clinopyroxene crystallites, and a trace of opaque minerals. There are about 7% vesicles up to 1.5 mm, some filled with yellow clays, and an altered mesostasis comprising about 37% of the rock. Clays are the predominant secondary minerals.

	J _{NRM}	MDF	Inc.	S	D	Rock Type
43-1, 146-148 cm	1.14x10 ⁻³	180	9.3	—	—	—
43-1, 146-150 cm	—	—	—	2.91	—	Alt. High-Mg andesite
43-2, 19-21 cm	1.36x10 ⁻³	175	9.7	—	—	—

60-458-44 3857.5-3867.0 m (408.5-418.0 m, BSF)

High-Mg bronzite andesite

Very intensely altered, fine- to medium-grained aphyric high-Mg bronzite andesite pillow basalt fragments. More or less coherent, but still fractured pieces were recovered at the top of the core, but the lower part of the core is very highly fractured. Pieces 3, 4, 6, 7, 8, 9, and 10 are greenish-black pillow rind fragments with spherulitic zones and abundant fractures. In all of these types of fragments, vesicles are usually empty or only partially filled with zeolite and/or clay. Pieces 1, 2, and 5 are massive fine-grained greenish-gray altered basalt. The highly fractured interval at the base of the core includes both pillow rim and pillow interior fragments.

	J _{NRM}	MDF	Inc.	S	D	Rock Type
44-1, 6-8 cm	2.00x10 ⁻³	186	12.3	—	—	—
44-1, 37-39 cm	1.06x10 ⁻³	550+	13.2	—	—	—
44-1, 71-73 cm	—	—	—	3.27	2.19	Alt. High-Mg andesite

60-458-45 3867.0-3876.5 m (418.0-427.5 m, BSF)

Aphyric basalt

Section 1: Pieces 1, 3, 9A, and 14-16 are fine-grained, dark greenish-gray, massive to slightly vesicular basalts, pervasively intensely altered to clays. Fractures are coated with smectites. Pieces 2, 9B-12 are highly vesicular (1-3 mm) greenish-black, variolitic, pillow rind fragments veined with zeolite and clay. Most vesicles are only partially filled with zeolites and clay. Pieces 3, 4, and 13 are fairly massive basalts with irregular vesicles (1-3 mm) that increase in abundance towards the vesicular pillow rinds above them.

Section 2: Piece 1 is an interval of breccia produced by drilling composed both of variolitic (pillow rind) and massive (pillow interior) fragments. Piece 2 is a massive fine-grained, dark greenish-gray slightly vesicular altered basalt. Piece 3 is a highly vesicular greenish-black fine-grained pillow rind fragment altered to zeolite and clays.

	J _{NRM}	MDF	Inc.	S	D	Rock Type
45-1, 117-119 cm	1.84x10 ⁻³	230	4.0	—	—	—
45-2, 29-31 cm	0.918x10 ⁻³	151	5.6	—	—	—
45-2, 70-74 cm	—	—	—	2.58	—	Alt. basalt

60-458-46 3876.5-3886.0 m (427.5-437.0 m, BSF)

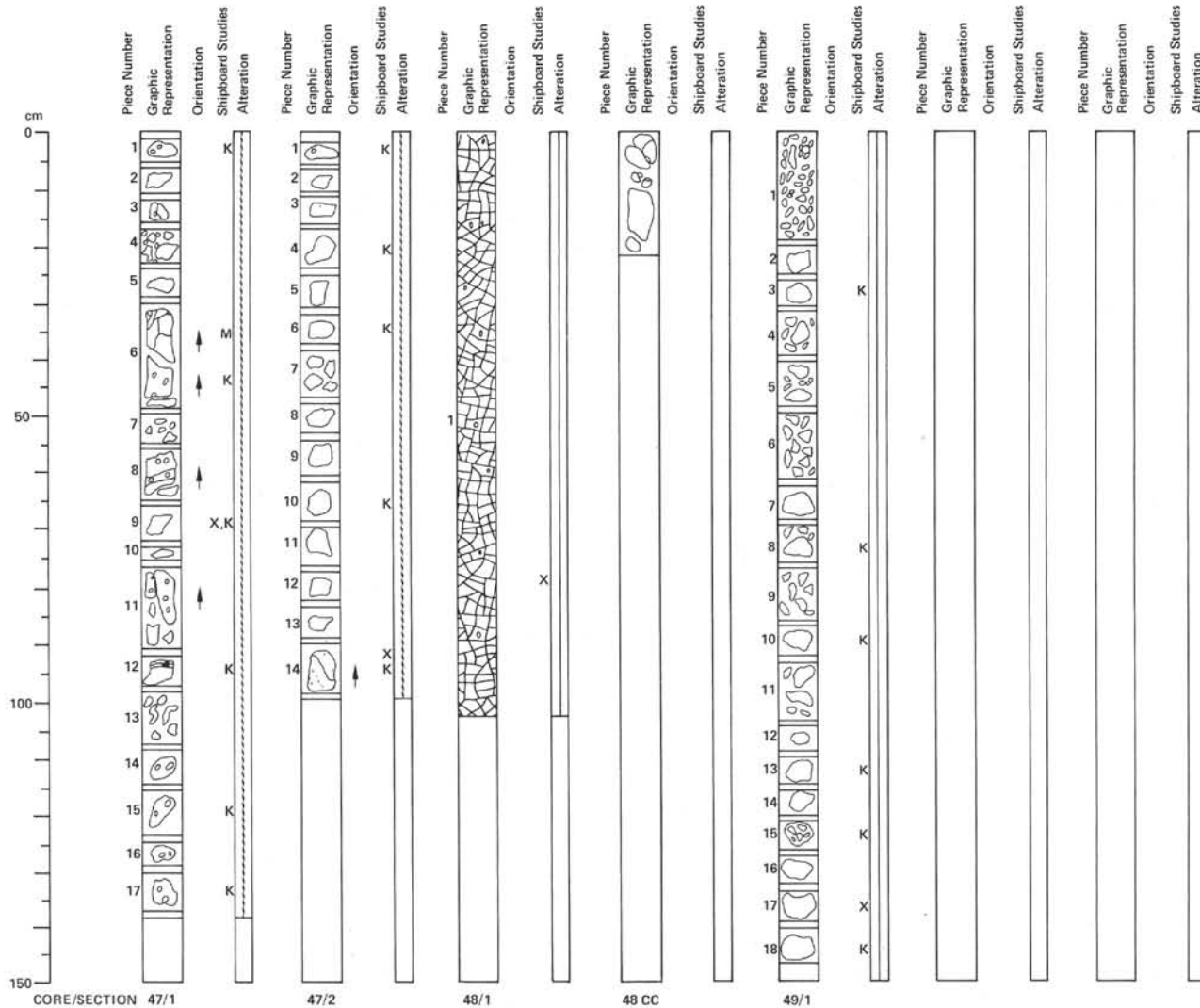
Aphyric basalt

Pieces 1-4 and 10 are fine-grained, sparsely vesicular, dark greenish-gray (5GY 4/1) fractured; pillow basalt fragments, altered to clay and in some instances, zeolite. Most vesicles are unfilled. Pieces 5-9 are fine-grained dark gray (N3) to greenish-black (5G 2/1), slightly vesicular, fractured basalts altered mainly to clays. Vesicles are generally not filled. Pieces 7-9 have 1.2 cm thick altered vertical and horizontal chilled glass rinds. These pieces of pillows are different from those in previous cores in that they have fewer vesicles and lack abundant zeolite veins and cavity fillings. They are also distinct chemically (Chemical Unit B₄).

Thin Section Description

46-1, 78-89 cm. Pilotaxitic basalt with a trace of euhedral plagioclase microphenocrysts (0.1-0.2 mm). The groundmass is about 10% acicular plagioclase with a fluidal alignment, a trace of skeletal clinopyroxene, and an altered mesostasis (once glass, now clays, and red Fe-hydroxides). Vesicles are rare (1%) and small (0.2-0.5 mm).

	J _{NRM}	MDF	Inc.	S	D	Rock Type
46-1, 85-87 cm	—	—	—	3.19	2.21	Alt. basalt
46-1, 88-90 cm	25.7x10 ⁻³	165	4.2	—	—	—



60-458-47 3886.0-3895.5 m (437.0-446.5 m, BSF)

Aphyric basalt

Fine-grained, dark greenish-gray to greenish-black, slightly vesicular (15-20%) aphyric basalt, altered to clay minerals and zeolite(?). Vesicles are occasionally aligned nearly horizontally. Fracture surfaces are coated with smectites. There is a glassy rim on Section 1, Piece 12, and in Section 2 there is a white vein mineral that seems harder than most zeolites. Veins in Section 2 are not coated with clay minerals.

	^J NRM	MDF	Inc.	S	D	Rock Type
47-1, 36-38 cm	10.7x10 ⁻³	151	-10.5	---	---	---
47-1, 81-83 cm	---	---	---	2.87	2.26	Alt. basalt

60-458-48 3895.5-3905.0 m (446.5-456.0 m, BSF)

Aphyric basalt

Extremely fractured and altered fine-grained, aphyric, aightly vesicular basalts. The rocks are very intensely altered. They are so soft they can easily be scratched with a fingernail. Fracturing and alteration nearly obliterate the original lithologic features (pillow rinds, etc.) of the basalts.

Thin Section Description

48-1, 69-71 cm. Pilotaxitic basalt with a trace of plagioclase (An₂₂) and clinopyroxene microphenocrysts. The groundmass is about 10% plagioclase (0.02-0.07 mm microlites), 6% clinopyroxene microlites, a trace of opaque minerals, and a highly altered devitrified glass mesostasis. Its color is now murky brown, and it is not translucent.

	^J NRM	MDF	Inc.	S	D	Rock Type
48-1, 39-41 cm	---	---	---	3.05	2.29	Alt. basalt

60-458-49 3905.0-3914.5 m (456.0-465.5 m, BSF)

Aphyric basalt

Disembled, mainly small (3-4 cm diameter), angular and subangular, fragments of fine-grained and badly altered dark greenish-gray (5GY 4/1) basalts with random spherical vesicles partly filled by chlorite(?), clay minerals, and zeolites. Many fragments have greenish-black (5GY 2/1) to grayish-blue green (5BG 5/2) slickensides, the result of brecciation. These features are typical of samples in the upper part of the core (Pieces 1-11). Pieces 12-18 are more massive, slightly rounded by drilling, and lack slickensides. Piece 15 resembles an altered hyaloclastite of a pillow margin. The other pieces are fine-grained greenish-black vesicular basalts.

	^J NRM	MDF	Inc.	S	D	Rock Type
49-1, 135-137 cm	---	---	---	3.20	2.24	Alt. basalt

